Engineering Structures 297 (2023) 116935

Contents lists available at ScienceDirect

Engineering Structures

journal homepage: www.elsevier.com/locate/engstruct

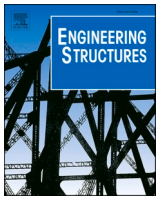

Stability and design of stainless steel hollow section columns at elevated temperatures

Chunyan Quan, Merih Kucukler *

School of Engineering, University of Warwick, Coventry CV4 7AL, UK

ARTICLE INFO

Keywords:
Column
Elevated temperature
Finite element modelling
Fire
Flexural buckling
Hollow section
Stainless steel

ABSTRACT

This paper investigates the stability and design of stainless steel circular, elliptical, square and rectangular hollow section (CHS, EHS, SHS and RHS) columns at elevated temperatures. Nonlinear shell finite element models are employed to conduct comprehensive parametric studies whereby extensive benchmark structural performance data on the behaviour and resistance of stainless steel hollow section columns at elevated temperatures is generated. In total, 26,760 cold-formed and hot-rolled austenitic, duplex and ferritic stainless steel CHS, EHS, SHS and RHS columns at elevated temperatures are taken into account, considering various member slendernesses, cross-section geometries, cross-section slendernesses and elevated temperature levels. New flexural buckling design rules are put forward for stainless steel hollow section columns in fire, which consistently considers the elevated temperature strength at 2% total strain $f_{2,\theta}$ as the reference material strength for all cross-sections classes. The accuracy, safety and reliability of the proposed new design rules are assessed for a wide range of cases. Comparisons are also made against the results obtained through the column fire design rules of the European structural steel fire design standard EN 1993-1-2 [1]. It is demonstrated that the proposed new design rules furnish more accurate, safe-sided and reliable flexural buckling resistance predictions for stainless steel hollow section columns at elevated temperatures relative to the column fire design provisions of EN 1993-1-2 [1].

1. Introduction

The use of stainless steel in the construction industry has been increasing as a result of its well-known advantages such as its excellent corrosion resistance, high durability and low maintenance requirements. Owing to its varied chemical composition, stainless steel exhibits different mechanical and thermal properties at elevated temperatures relative to carbon steel, resulting in superior strength and stiffness retention in fire [2]. However, in the current version of the European structural steel fire design standard EN 1993-1-2 [1], the design rules for stainless steel structural elements are largely based upon those originally developed for carbon steel elements, leading to an inconsistent design treatment of the actual behaviour of stainless steel structures in fire [3]. For the purpose of addressing this issue, a number of research studies have recently been carried out, aiming to specifically investigate the behaviour and design of stainless steel structures at elevated temperatures.

Ng and Gardner [4] investigated the structural behaviour of stainless steel columns and beams in fire through numerical analysis and recommended modifications to EN 1993-1-2 [1] design rules. In [4], it is recommended that the cross-section and member resistances of stainless steel columns in fire can be determined using the elevated temperature material strength at 2% total strain $f_{2,\theta}$ for Class 1 and 2 cross-sections and the elevated temperature 0.2% proof strength $f_{p0.2,\theta}$ for Class 3 and 4 cross-sections. In [5,6], numerical parametric studies were performed on austenitic, duplex and ferritic stainless steel circular hollow section (CHS) and elliptical hollow section (EHS) columns at elevated temperatures, where it was observed that the ultimate resistances predicted using EN 1993-1-2 [1] are either overly-conservative or quite unsafe for some cases. Assessment of the fire design methods proposed in [1,7,8] was carried out in [5,6]; however, no modification of the design methods put forward in [1,7,8] to increase their accuracy was recommended. Fan et al. [9] conducted fire experiments on eight austenitic stainless steel square hollow section (SHS) columns and beam-columns and also performed a numerical study on stainless steel SHS columns at elevated temperatures [10], concluding that EN 1993-1-2 [1] provides conservative results. Calibrated against experimental and numerical data, new buckling curves for stainless steel SHS columns in fire

* Corresponding author.
E-mail address: merih.kucukler@warwick.ac.uk (M. Kucukler).

https://doi.org/10.1016/j.engstruct.2023.116935
Received 25 April 2023; Received in revised form 15 July 2023; Accepted 20 September 2023
Available online 7 October 2023

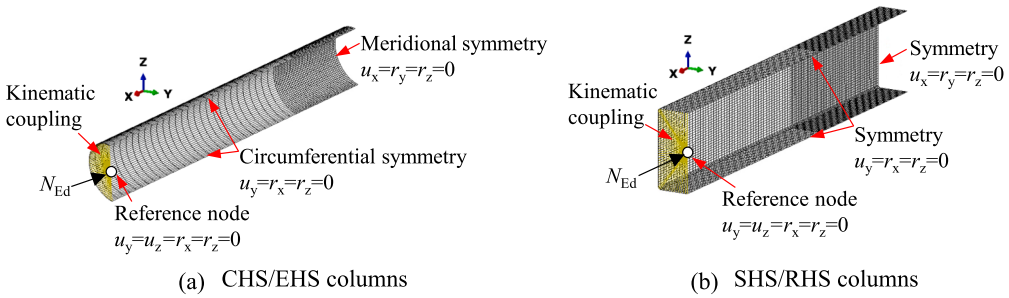

Fig. 1. Details of finite element models developed in this study.

were put forward in [10], which adopted $f_{2,\theta}$ as the reference material strength for Class 1–3 (non-slender) cross-sections and $f_{p0.2,\theta}$ for Class 4 (slender) cross-sections. Lopes et al. [7] performed numerical studies on welded stainless steel I-section columns in fire. Observing the inaccuracy of the column fire design rules of EN 1993-1-2 [1], Lopes et al. [7] proposed a modification to the existing column fire design rules provided in EN 1993-1-2 [1], which also adopted $f_{2,\theta}$ as the reference material strength for Class 1–3 cross-sections and $f_{p0.2,\theta}$ for Class 4 cross-sections. The design method of [7] which was originally developed for I-section columns was extended in [11] to also cover the design of cold-formed stainless steel hollow section columns, but only considering non-slender cross-sections.

The adoption of $f_{2,\theta}$ for the fire design of Class 1, 2 and 3 sections and $f_{p0.2,\theta}$ for Class 4 sections results in artificial steps in the resistance predictions between Class 3 and Class 4 cross-sections. Additionally, Couto et al. [12] observed that this adoption leads to conservative resistance predictions for Class 4 cross-sections, particularly for cross-sections with both slender and non-slender plate elements. To eliminate these shortcomings, Couto et al. [12] recommended the consistent use of $f_{2,\theta}$ as the reference material strength for all cross-section classes in the determination of the ultimate resistances of steel cross-sections in fire. In line with [12], Kucukler et al. [8] performed parametric studies on welded stainless steel I-section columns at elevated temperatures and proposed a new design method which consistently considers $f_{2,\theta}$ as the reference strength for the fire design of stainless steel columns regardless of their cross-section class; it is demonstrated that the new design method of [8] provides more accurate resistance predictions relative to EN 1993-1-2 [1]. The fire design method of [8] is due to be included in the upcoming version of EN 1993-1-2 [1] which is currently referred to as prEN 1993-1-2 [13]. However, the fire design method of [8] was originally developed considering the structural response of welded stainless steel I-section columns at elevated temperatures only and may not be suitable for stainless steel hollow section columns at elevated temperatures [6,14].

With the aim of both understanding and accurately estimating the structural response of stainless steel hollow sections at elevated temperatures, this paper presents a comprehensive research study on the flexural buckling behaviour and design of stainless steel hollow section columns at elevated temperatures, taking into consideration traditional stainless steel hollow sections, such as CHS, SHS and rectangular hollow section (RHS) columns in fire. Recently, elliptical hollow sections (EHS) have attracted considerable attention from designers and researchers since they exhibit high structural efficiency due to the different flexural stiffnesses in two principal axes but still retain the aesthetic appearance of hollow sections [15–17]. Thus, stainless steel EHS columns are also taken into consideration in this study. Since different manufacturing processes (cold-formed and hot-rolled) may exhibit different material responses and result in different structural behaviour [18–20], both cold-formed and hot-rolled stainless steel cross-sections are considered in this study. Although hot-rolled structural stainless steel hollow sections are less common relative to cold-formed stainless steel hollow sections, such sections have been introduced to the industry [21,22]; thus, for the sake of completeness and taking into account their possible use in future, hot-rolled stainless steel hollow sections are also considered in this study. Comprehensive numerical parametric studies are performed on stainless steel hollow section columns by means of nonlinear shell finite element (FE) modelling, taking into account austenitic, duplex and ferritic stainless steel grades, various member slendernesses, cross-section geometries, cross-section slendernesses and different elevated temperature levels. In total, the structural response of 26,760 stainless steel hollow section columns in fire was considered. Calibrated against the benchmark shell FE results, new flexural buckling curves for the design of stainless steel hollow section columns at elevated temperatures are proposed. The accuracy and reliability of the proposed new design rules are assessed against the benchmark FE results as well as the resistance estimations from the existing fire design provisions of EN 1993-1-2 [1]. The higher accuracy and consistency of the proposed design rules relative to the design provisions of EN 1993-1-2 [1] are demonstrated.

2. Finite element modelling

In this study, shell elements in Abaqus [23] are utilised to simulate the flexural buckling behaviour of stainless steel hollow section columns at elevated temperatures. Geometrically and Materially Nonlinear Analyses with Imperfections (GMNIA) are performed through nonlinear shell FE models to generate benchmark structural performance data, whereby a new fire design method for stainless steel hollow section columns is calibrated and established. In this section, the development of the shell FE models is described. After their validation against experimental results from the literature, the developed shell FE models are used to perform extensive numerical parametric studies.

2.1. Development of finite element models

2.1.1. Modelling approach

The FE analysis software Abaqus [23] was employed to perform numerical simulations. The general-purpose four-noded shell finite element with reduced integration S4R was utilised in the FE modelling, which has been successfully employed in previous studies for similar applications [24,25]. Employing suitable boundary conditions for CHS/EHS and SHS/RHS columns, (i) a symmetry plane was exploited at the midspan and (ii) another symmetry plane was also exploited along the two longitudinal edges through the member length, thereby producing computationally efficient quarter models as shown in Fig. 1. The generated quarter FE models have been verified against the results obtained from the counterpart full FE models. The displacements and rotations at the end sections were linked to a reference node through kinematic coupling. Pin-ended boundary conditions about the buckling axis were established at the reference node by releasing the rotation about the buckling axis (i.e. $u_y = u_z = r_x = r_z = 0$, but $r_y \neq 0$). The concentric axial force N_{Ed} was also applied to this reference node.

For CHS and EHS columns, a fine mesh with shell element size of $0.1\sqrt{D_e t}$ was adopted, where t is the cross-section thickness and D_e is the

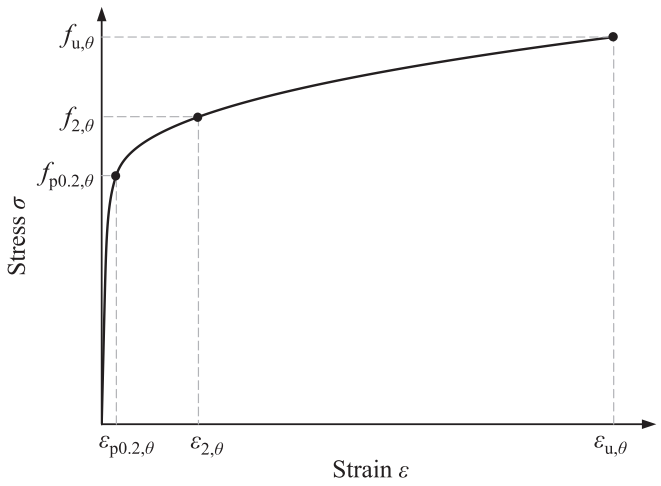

Fig. 2. Two-stage elevated temperature Ramberg-Osgood material model for stainless steel [38–40].

equivalent diameter. D_e is equal to the outer diameter D for CHS and equal to $D[1 + (1 - 2.3(t/D)^{0.6})(D/B - 1)]$ for EHS [26,27], where D and B are the larger and smaller outer diameters, respectively. For the purpose of achieving computational efficiency in the numerical simulations, this fine mesh was only applied within the midspan region along the member length whose length was taken six times of the elastic local buckling half-wavelength of the cross-section in accordance with [28]. For this region, the element size was chosen such that the element aspect ratios were approximately equal to unity, while for the remainder of the modelled columns, a coarser mesh with the element size of $0.5\sqrt{D_e t}$ was used in line with the approach adopted in [28]. This meshing strategy has been shown to be sufficiently refined to provide accurate estimations of the local buckling behaviour of CHS and EHS members [28,29]. For SHS and RHS elements, to avoid corner crackling during the cold-rolling procedure, cold-formed SHS/RHS generally have larger radii than hot-rolled SHS/RHS [30,31]. In this study, the external corner radii r provided in EN 10219-2 [32] and EN 10210-2 [33] were adopted. Thus, the external corner radii r were taken as $2t$ for cold-formed SHS/RHS and $1.5\,t$ for hot-rolled SHS/RHS, where t is the cross-section thickness. To accurately capture the elastic–plastic member behaviour, a fine mesh with shell element size equal to the cross-section thickness t was employed within the flat regions of SHS/RHS columns, while four elements were employed in the corner regions in line with [34]. Adopting a similar approach to that used in the shell FE models of the CHS/EHS columns, the fine mesh was only applied to the midspan region whose length was taken equal to four times of the overall cross-section height H in accordance with [35]. In the midspan region, the element size along the member length was selected such that the aspect ratios of the elements were approximately equal to unity; while for the remainder of the modelled SHS/RHS columns, a coarser mesh with the element size equal to two times of that of the fine mesh was employed in accordance with the procedure adopted in [35]. The Simpson integration method was employed and five integration points were used through the thickness of the shell elements [23]. In the FE simulations, the isothermal analysis technique was adopted in line with the previous research [36,37] where (i) the temperatures of stainless steel columns were first increased to prescribed levels θ and (ii) then, the axial compression was applied at the specified elevated temperature levels θ which remained constant during the load application. The modified Riks analysis [23] was adopted to capture the full load-deformation response of the modelled columns including the post-ultimate paths, whereby the highest values of the applied axial compression observed in the simulations were taken as the ultimate load carrying capacities of the stainless steel hollow section columns at elevated temperatures.

2.1.2. Material modelling

Both cold-formed and hot-rolled stainless steel hollow section columns were taken into consideration in this paper. For each stainless steel family, one typical grade was selected: 1.4301 austenitic (A), 1.4462 duplex (D) and 1.4003 ferritic (F). In this study, the two-stage Ramberg-Osgood material model [38–40] was used to express the full stress–strain σ-ε response at temperature θ, as given by Eqs. (1)–(2) and illustrated in Fig. 2, where E_θ is the Young's modulus at temperature θ, $E_{p0.2\theta}$ is the tangent modulus at the 0.2% proof stress $f_{p0.2,\theta}$ as given by Eq. (3), $\varepsilon_{p0.2,\theta}$ is the total strain at $f_{p0.2,\theta}$ equal to $0.002 + f_{p0.2,\theta}/E_\theta$, $f_{u,\theta}$ and $\varepsilon_{u,\theta}$ are the ultimate strength and strain at temperature θ, and n_θ and m_θ are the strain hardening exponents, respectively.

$$\varepsilon = \frac{\sigma}{E_\theta} + 0.002\left(\frac{\sigma}{f_{p0.2,\theta}}\right)^{n_\theta} \quad \text{for } \sigma \leqslant f_{p0.2,\theta} \tag{1}$$

$$\varepsilon = \varepsilon_{p0.2,\theta} + \frac{\sigma - f_{p0.2,\theta}}{E_{p0.2,\theta}} + \left(\varepsilon_{u,\theta} - \varepsilon_{p0.2,\theta} - \frac{f_{u,\theta} - f_{p0.2,\theta}}{E_{p0.2,\theta}}\right)\left(\frac{\sigma - f_{p0.2,\theta}}{f_{u,\theta} - f_{p0.2,\theta}}\right)^{m_\theta} \quad \text{for } f_{p0.2,\theta} < \sigma \leqslant f_{u,\theta} \tag{2}$$

$$E_{p0.2,\theta} = \frac{E_\theta}{1 + 0.002 n_\theta \frac{E_\theta}{f_{p0.2,\theta}}} \tag{3}$$

The material properties at elevated temperatures (i.e. $f_{p0.2,\theta}$, $f_{2,\theta}$, $f_{u,\theta}$, $\varepsilon_{u,\theta}$, E_θ) utilised in Eqs. (1)–(3) were determined by multiplying the material properties at room temperature, i.e. the yield (0.2% proof) stress f_y, ultimate stress f_u, ultimate strain ε_u and Young's modulus E, by the corresponding strength ($k_{p0.2,\theta}$, $k_{2,\theta}$, $k_{u,\theta}$), ductility ($k_{\varepsilon u,\theta}$) and stiffness ($k_{E,\theta}$) reduction factors provided in Steel Construction Institute (SCI) Design Manual for Structural Stainless Steel [41], which are based on the results from the elevated temperature material tests on stainless

Table 1
Overview of adopted standardised material parameters for the FE models [46].

Type	Grade	Young's modulus E (N/mm^2)	Yield (0.2% proof) stress f_y (N/mm^2)	Ultimate stress f_u (N/mm^2)	Ultimate strain ε_u	Strain hardening exponent n
Cold-formed stainless steel SHS/RHS (flat region) and CHS/EHS	Austenitic (A)	200,000	460	700	0.20	7.1
	Duplex (D)		630	780	0.13	7.5
	Ferritic (F)		430	490	0.06	11.5
Cold-formed stainless steel SHS/RHS (corner region)	Austenitic (A)	200,000	640	830	0.20	6.4
	Duplex (D)		800	980	0.03	6.1
	Ferritic (F)		560	610	0.01	5.7
Hot-rolled stainless steel	Austenitic (A)	200,000	280	580	0.50	9.1
	Duplex (D)		530	770	0.30	9.3
	Ferritic (F)		320	480	0.16	17.2

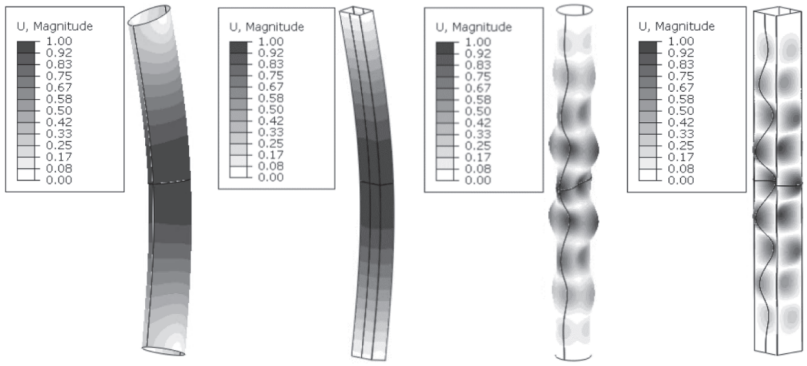

(a) Major axis global buckling of EHS (b) Minor axis global buckling of RHS (c) Local buckling of CHS (d) Local buckling of SHS

Fig. 3. Typical elastic buckling modes of hollow section columns from LBA.

steel grades reported in [42–45], thus $f_{p0.2,\theta} = k_{p0.2,\theta} f_y$, $f_{2,\theta} = k_{2,\theta} f_y$, $f_{u,\theta} = k_{u,\theta} f_u$, $\varepsilon_{u,\theta} = k_{\varepsilon u,\theta} \varepsilon_u$ and $E_\theta = k_{E,\theta} E$. Note that the described material reduction factors adopted in this study will appear in prEN 1993-1-2 [13] in conjunction with the two stage Ramberg-Osgood material model given by Eqs. (1)–(2) for the elevated temperature material modelling of stainless steel. Thus, the elevated temperature material modelling approach employed in this study is fully in accordance with prEN 1993-1-2 [13]. The standardised room temperature material properties recommended in [46] for cold-formed and hot-rolled stainless steel cross-sections, which were derived on the basis of the analysis of a comprehensive database of material tests for different stainless steel products, were employed in this study, as provided in Table 1.

For cold-formed stainless steel CHS/EHS and all the considered hot-rolled stainless steel cross-sections, the material properties were uniformly applied to the cross-sections. On the other hand, for cold-formed stainless steel SHS/RHS, due to the different extents of plastic deformations within the cross-sections during production, further strength enhancements arise in the corner regions [47,48]. To consider these strength enhancements in the cold-formed stainless steel SHS/RHS columns, enhanced material properties were assigned to the corner regions plus extensions of $2t$ into the flat regions [48,49]. On the basis of the results from elevated temperature material tests, [50,51] concluded that the enhanced material strengths due to cold-working can be maintained at elevated temperatures (up to 700 °C). The use of the elevated temperature material reduction factors with the enhanced material strengths for cold-formed stainless steel cross-sections is also recommended in the upcoming version of the European structural steel fire design standard prEN 1993-1-2 [13]. Thus, in this study, in line with the recommendations in [13,41,44,51], the same elevated temperature reduction factors were utilised for cold-formed and hot-rolled stainless steel cross-sections at the considered temperature levels 300–700 °C, but with different room temperature material properties, which result in different elevated temperature material response.

In line with the recommendations of [13,41], the values of the first strain hardening exponents n_θ used to define the roundedness of the first stage of the elevated temperature material response were taken equal to their room temperature values n, which are provided in [46] and listed in Table 1. For the second strain hardening exponents m_θ used to define the roundedness of the second stage of the elevated temperature material response, the values calculated using Eq. (4) [13] were employed, thereby ensuring that the second stage of the two-stage Ramberg-Osgood material model exactly passes through $f_{2,\theta}$ at 2% total strain $\varepsilon_{2,\theta}$ and $f_{u,\theta}$ at the ultimate strain $\varepsilon_{u,\theta}$.

$$m_\theta = \frac{\ln\left(\frac{0.02-\varepsilon_{p0.2,\theta}-\frac{f_{2,\theta}-f_{p0.2,\theta}}{E_{p0.2,\theta}}}{\varepsilon_{u,\theta}-\varepsilon_{p0.2,\theta}-\frac{f_{u,\theta}-f_{p0.2,\theta}}{E_{p0.2,\theta}}}\right)}{\ln\left(\frac{f_{2,\theta}-f_{p0.2,\theta}}{f_{u,\theta}-f_{p0.2,\theta}}\right)} \text{ but } 1.5 \leqslant m_\theta \leqslant 5 \quad (4)$$

In Quan and Kucukler [52], the stress–strain curves employed in this study were compared against the elevated temperature test results on grade 1.4301 austenitic, 1.4462 duplex and 1.4016 ferritic stainless steel coupons; the results demonstrated that the adopted material modelling is able to represent the elevated temperature material response of stainless steel coupons obtained from the elevated temperature material tests.

2.1.3. Initial imperfections

Global geometric imperfections were incorporated into the shell FE models by using global buckling modes from the Linear Buckling Analyses (LBA) and scaling the modes by amplitudes equal to $L/1000$ where L is the member length. Local geometric imperfections were also incorporated into the shell FE models by scaling the lowest elastic local buckling modes obtained from the LBA. Note that in the application of the local imperfections to CHS/EHS columns, to effectively preclude the use of inappropriate elastic local buckling shapes with unrealistically short local buckling half-wavelengths, the LBA were performed on the FE models with a modified thickness of $t_{mod} = D/5$ for CHS and $t_{mod} = B/5$ for EHS in line with the approach adopted in [28]. In accordance with the recommendations of Annex C of EN 1993-1-5 [53], the local imperfection amplitudes were taken as 80% of the geometric fabrication tolerances, which are provided in EN 10219-2 [32] for cold-formed steel hollow sections and EN 10210-2 [33] for hot-rolled steel hollow sections. Thus, for CHS and EHS, the geometric fabrication tolerance value was taken as $D/100$ but between 0.5 mm and 10 mm. For SHS and RHS, the geometric fabrication tolerance value was taken as $H/100$ but no less than 0.5 mm. Fig. 3 presents the typical elastic local and global buckling modes of hollow section columns obtained from LBA. The global and local geometric imperfections were applied in the most unfavourable directions, i.e. the local imperfections at the mid-height were inward at the concave side of the globally imperfect shapes [54].

In hot-rolled stainless steel hollow sections, residual stresses are shown to be negligible [21]. In cold-formed stainless steel hollow sections, membrane residual stresses are also deemed to be very small, while the effect from the dominant bending residual stresses is implicitly incorporated into measured stress–strain curves [55,56]. Thus, in this study, residual stresses were not incorporated into the shell FE models in line with the previous studies on the behaviour of steel and stainless steel structural members in fire [11,27,57,58].

2.2. Validation of numerical models

The shell FE models developed in this study were validated against the results from physical tests on steel and stainless steel hollow section columns from the literature [9,59–62], including 37 room temperature tests and 15 anisothermal fire tests. The geometric properties, material properties, boundary conditions and loading conditions of the shell FE

Table 2
Validation of shell FE models against test results of stainless steel CHS columns [59].

Grade	Section	No.	$N_{u,FE}/N_{u,test}$			
			Mean	CoV	Max	Min
A	CHS 106 × 3	9	0.92	0.039	0.98	0.86
A	CHS 104 × 2	8	0.98	0.099	1.09	0.85
D	CHS 88.9 × 2.6	9	1.04	0.062	1.13	0.95
F	CHS 80 × 1.5	6	1.03	0.041	1.11	0.97
F	CHS 101.6 × 1.5	5	1.07	0.070	1.19	1.00
Total		37	1.00	0.087	1.19	0.85

models were consistent with those employed in the experiments.

Currently, there are very few fire tests on steel or stainless steel CHS columns in the literature and the fire experiments on high-strength steel CHS columns performed by Tondini et al. [63] have been utilised to validate the shell FE modelling approach in Quan and Kucukler [64]; note that the same shell FE modelling approach used in [64] was adopted in this study and thus, the validation study provided in [64] also underpins the accuracy of the shell FE models used in this paper. Considering that the experimental results from Tondini et al. [63] were used for the validation of the shell FE modelling in another study, in this paper, the room temperature experiments on stainless steel CHS columns performed by [59] were adopted for the further validation of the shell FE modelling approach. As summarised in Table 2, 37 pin-ended austenitic, duplex and ferritic stainless steel CHS column tests were carried out in [59], considering 5 different CHS geometries. The mean, coefficient of variation (CoV), maximum and minimum values of the ratios of the ultimate member resistances obtained from the shell FE models $N_{u,FE}$ to those observed in the experiments $N_{u,test}$ (i.e. $N_{u,FE}/N_{u,test}$) for each section group are shown in Table 2. Fig. 4 presents the axial load versus midspan deflection paths obtained from the experiments and shell FE models for stainless steel CHS columns labelled as 106 × 3-1650-P, 106 × 3-3080-P, 88.9 × 2.6-950-P, 88.9 × 2.6-2650-P, 104 × 2-1650-P, 104 × 2-2650-P, 80 × 1.5-700-P and 80 × 1.5-1100-P from the tests in [59]. It can be seen from the Table 2 and Fig. 4 that the developed shell FE models provide load-deformation curves and ultimate member resistances close to those observed in the physical tests, providing a further illustration of the accuracy of the adopted shell FE modelling approach in replicating the structural response of stainless steel CHS columns.

Additionally, the developed shell FE models were also validated against the anisothermal fire tests performed on (i) 6 pin-ended steel EHS columns [60,61], (ii) 6 pin-ended austenitic stainless steel SHS

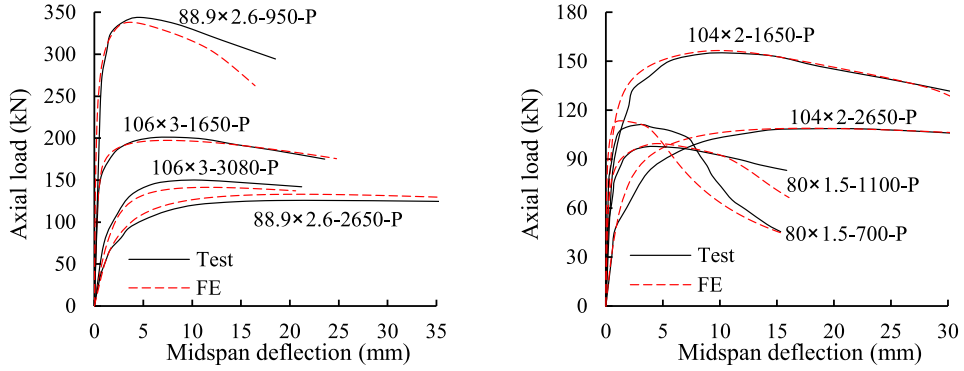

(a) CHS 106×3 and 88.9×2.6 (b) CHS 104×2 and 80×1.5

Fig. 4. Comparison of the axial load versus midspan deflection paths obtained from experiments and shell FE models for stainless steel CHS columns at room temperature [59].

Table 3
Validation of shell FE models against results of anisothermal experiments for steel EHS and stainless steel SHS columns from literature [9,60–62].

Reference	Test	Grade	Section	L mm	N kN	θ_{test} °C	θ_{FE} °C	$\theta_{FE}/\theta_{test}$
Scullion et al. (2011)	A1	S355	EHS 250 × 125 × 8	1800	800	389	426	1.10
	A2		EHS 250 × 125 × 8	1800	600	504	496	0.98
	A3		EHS 250 × 125 × 8	1800	400	586	563	0.96
	B1		EHS 200 × 100 × 8	1800	600	460	470	1.02
	B2		EHS 200 × 100 × 8	1800	450	519	524	1.01
	B3		EHS 200 × 100 × 8	1800	300	597	586	0.98
Fan et al. (2016)	Z1	A	SHS 100 × 100 × 4	3300	85	>742	781	<1.05
	Z2		SHS 100 × 100 × 4	3300	120	720.8	721	1.00
	Z3		SHS 100 × 100 × 4	3300	152	642.4	615	0.96
	Z4		SHS 120 × 120 × 4	3300	132	793	786	0.99
	Z5		SHS 120 × 120 × 4	3300	184	723	734	1.02
	Z6		SHS 120 × 120 × 4	3300	236	593	620	1.05
Tondini et al. (2013)	C1	F	SHS 80 × 80 × 3	3000	72	709	709	1.00
	C2		SHS 80 × 80 × 3	2500	78	708	702	0.99
	C3		SHS 120 × 100 × 3	2500	100	705	710	1.01
Total								15
Mean								1.01
CoV								0.035
Max								1.10
Min								0.96

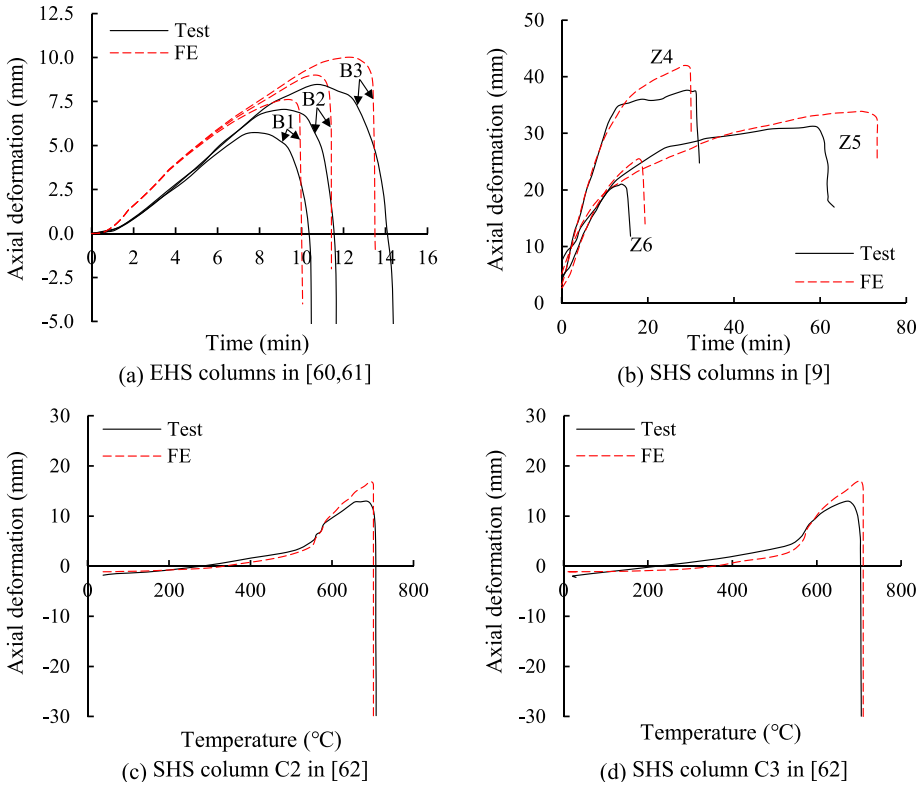

Fig. 5. Comparison of the axial deformation versus time or temperature paths obtained from the anisothermal experiments and shell FE models for S355 steel EHS columns in [60,61], austenitic stainless steel SHS columns in [9] and ferritic stainless steel SHS columns in [62].

Table 4
Summary of parametric studies on cold-formed and hot-rolled stainless steel CHS/EHS and SHS/RHS columns.

Cross-section	Material	θ (°C)	Aspect ratio	Cross-section slenderness	Member slenderness
CHS	Cold-formed and hot-rolled	300	D/B = 1	$(D/t)(f_y/235)$ = 20, 45, 110, 175, 240	L/D = 5 to 50 with Δ5
EHS	A	400	D/B = 1.5, 2, 2.5	$(D_e/t)(f_y/235)$ = 40, 60, 120, 180, 240	L/D = 5 to 50 with Δ5 (Major axis)
	D	500			
	F	600			
		700			
					L/B = 5 to 50 with Δ5 (Minor axis)
SHS			H/B = 1	$\bar{\lambda}_{p,H}$ = 0.25, 0.4, 1, 1.5, 2	L/H = 5 to 50 with Δ5
RHS			H/B = 1.25, 1.67, 2		L/H = 5 to 50 with Δ5 (Major axis)
					L/B = 5 to 50 with Δ5 (Minor axis)

columns [9] and (iii) 3 pin-ended ferritic stainless steel SHS columns [62]. In the anisothermal tests, prescribed axial loads were applied to the specimens first and kept constant, and then the temperatures were increased until failure. The test number, material grade, section profile, member length L, the applied axial load N and comparisons between the numerical critical temperatures θ_{FE} and the experimental critical temperatures θ_{test}, as well as the mean, CoV, maximum and minimum values of the ratios $\theta_{FE}/\theta_{test}$ are presented in Table 3. It can be seen from the table that the critical temperature predictions obtained from the developed shell FE models are generally close to those observed in the fire experiments. Fig. 5 presents comparisons between the axial deformation versus time or temperature paths obtained from the anisothermal fire experiments and those obtained from the shell FE models created herein for (i) the grade S355 steel EHS columns labelled as B1, B2 and B3 from the fire tests carried out in [60,61], (ii) the austenitic stainless steel SHS columns labelled as Z4, Z5 and Z6 from the fire tests in [9] and (iii) the ferritic stainless steel SHS columns labelled as C2 and C3 from the fire experiments performed in [62]. As can be seen from Fig. 5, the numerical curves generally agree well with the experimental curves. In Fig. 5 (a), the initial stiffnesses of the deformation-time curves obtained from the FE models are somewhat different than those observed in the experiments [60], which was also observed in [61] during the validation of the numerical models created in [61] against the experiments of [60]. In [61], the reason behind this was ascribed to the slackness and bedding within the test rig at the beginning of the heating process which led to the delays in the measurement of the axial deformations in the experiments until the steel temperature was approximately 100 °C. However, as can be seen from Fig. 5, there is a good correlation between the overall axial deformation versus time paths observed in the experiments and those obtained through the shell FE models herein, thus verifying the accuracy of the adopted FE modelling approach which has also been extensively validated in previous studies [52,64]. The validation studies carried out in this subsection indicate that the adopted FE modelling approach is able to accurately replicate

Table 5
Limits for the classification of stainless steel CHS/EHS and SHS/RHS at elevated temperatures according to EN 1993-1-2 [1] and EN 1993-1-4 [66].

Cross-section	Limit	Class 1	Class 2	Class 3
CHS/EHS	Equivalent diameter-to-thickness ratio D_e/t	$50\varepsilon_\theta^2$	$70\varepsilon_\theta^2$	$90\varepsilon_\theta^2$
SHS/RHS	Width-to-thickness ratio of flat regions $(H\text{-}2r)/t$	$33\varepsilon_\theta$	$35\varepsilon_\theta$	$37\varepsilon_\theta$

the behaviour of stainless steel CHS/EHS and SHS/RHS columns at elevated temperatures and can be used to generate benchmark data in further parametric studies, whereby the new flexural buckling design rules for stainless steel hollow section columns at elevated temperatures can be established.

2.3. Parametric study

Upon the validation of the employed shell FE modelling approach, parametric studies were conducted to generate benchmark structural performance data. Table 4 summaries the parameters taken into account in the numerical parametric studies on stainless steel CHS/EHS and SHS/RHS columns at elevated temperatures. Both cold-formed and hot-rolled austenitic, duplex and ferritic stainless steel were considered, covering major or minor axis flexural buckling cases. Isothermal analyses were performed on stainless steel columns, taking into consideration 5 different elevated temperature levels θ equal to 300 °C, 400 °C, 500 °C, 600 °C and 700 °C, corresponding to typical critical temperature levels in stainless steel structural elements [5], which was also in line with the elevated temperature ranges considered in previous similar studies [6,25].

The outer diameters D of CHS, the larger outer diameters D of EHS and the overall cross-section depths H of SHS and RHS were taken as a contant value equal to 100 mm in all the considered cases in the numerical parametric studies. The aspect ratios D/B of the studied EHS were taken as 1.5, 2 and 2.5; on the other hand, the aspect ratios H/B of the studied RHS were taken as 1.25, 1.67 and 2, where H and B are the cross-section depth and width, respectively. The cross-section thicknesses t were varied to achieve a broad spectrum of cross-section slendernesses. For CHS, the cross-section thicknesses t were determined using the parameter $(D/t)(f_y/235)$ which were taken equal to 20, 45, 110, 175 and 240. For EHS, the cross-section thicknesses t were determined using a similar parameter $(D_e/t)(f_y/235)$ which were taken equal to 40, 60, 120, 180 and 240. The normalised material strength factor $(f_y/235)$ was adopted in the variations of the thicknesses of CHS and EHS herein so as to take into account the influence of different material strengths on the cross-sectional behaviour in accordance with the use of $(f_y/235)$ in the cross-section classification rules of EN 1993-1-1 [65] and EN 1993-1-4 [66]. Note that a higher lower limit was adopted for $(D_e/t)(f_y/235)$ ratios in the EHS cases to avoid unrealistic thicknesses for high cross-section aspect ratios D/B. For SHS/RHS, the cross-section thicknesses t were varied such that the plate slendernesses of the wider flat portions of the stainless steel SHS/RHS $\bar{\lambda}_{p,H}$ were equal to 0.25, 0.4, 1, 1.5 and 2. Of course, the influence from the material strengths is directly considered through the plate slendernesses $\bar{\lambda}_{p,H}$.

For the CHS columns and EHS columns subjected to major axis buckling, the ratios of L/D were ranged between 5 and 50 with an increment of 5; on the other hand, for the EHS columns subjected to minor axis buckling, the ratios of L/B were ranged between 5 and 50 with an increment of 5. Similarly, for the SHS columns and RHS columns subjected to major axis buckling, the ratios of L/H were ranged between 5 and 50 with an increment of 5, while for the RHS columns subjected to minor axis buckling, the ratios of L/B were ranged between 5 and 50 with an increment of 5.

3. EN 1993-1-2 column fire design method

In this section, the fire design rules of EN 1993-1-2 [1] for stainless steel columns are briefly introduced. According to EN 1993-1-2 [1], the influence of flexural buckling on the resistance of a stainless steel column in fire is taken into account by the application of a buckling reduction factor to the cross-section compression resistance which is determined by considering the cross-section class and local buckling assessment rules. In Section 3.1, the cross-section classification system employed in EN 1993-1-2 [1] is described, while the calculation of the cross-section compression resistances based on the corresponding cross-section classes is introduced in Section 3.2. Following this, the application of the buckling reduction factors determined using a flexural buckling curve to the cross-section resistances is presented in Section 3.3. The accuracy of the EN 1993-1-2 [1] fire design rules for stainless steel hollow section columns is assessed in Section 5.

3.1. Cross-section classification

For the classification of stainless steel cross-sections in fire, EN 1993-1-2 [1] directs the designers to the cross-section classification rules provided in the European room temperature structural stainless steel design standard EN 1993-1-4 [66] but recommends their use with a reduced elevated temperature material factor ε_θ, which is determined using the room temperature material factor ε, as given by Eq. (5).

$$\varepsilon_\theta = 0.85\varepsilon = 0.85\sqrt{\frac{235}{f_y}\frac{E}{210000}} \tag{5}$$

According to EN 1993-1-2 [1] and EN 1993-1-4 [66], stainless steel cross-sections are classified into four classes at elevated temperatures. Table 5 summarises the limits for the classification of stainless steel CHS/EHS and SHS/RHS in fire according to EN 1993-1-2 [1] and EN 1993-1-4 [66]. For CHS and EHS, the ratio of the equivalent diameter D_e (see Section 2.1.1) to the cross-section thickness t (i.e. D_e/t) is adopted to determine the cross-section class, while the width-to-thickness ratios of the internal plate elements are used in the cross-section classification of SHS and RHS. In the cross-section classification, the employed plate widths of the cross-section elements of SHS and RHS are taken as the widths of the flat regions excluding the rounded corners. Thus, for SHS/RHS subjected to pure axial compression, the $(H\text{-}2r)/t$ ratio is used for the determination of the cross-section class.

In line with the Steel Construction Institute (SCI) Design Manual for Structural Stainless Steel [41], to account for the beneficial effects from the strength enhancements in the corner regions of cold-formed SHS and RHS, the average yield strength $f_{y,ave}$ can be adopted to determine their design cross-section resistances, as given by:

$$f_{y,ave} = \frac{f_{y,corner}A_{corner} + f_{y,flat}(A - A_{corner})}{A} \tag{6}$$

in which $f_{y,corner}$ and $f_{y,flat}$ are the yield strengths of corner regions and flat regions and A_{corner} is the total corner cross-sectional area including the extensions of 2 t into the flat regions. If the average yield strength $f_{y,ave}$ is adopted for the determination of the design elevated temperature cross-section resistance, the cross-section classification should also be carried out using the elevated temperature material factor $\varepsilon_{ave,\theta}$ based on $f_{y,ave}$ as determined by Eq. (7) in line with the upcoming version of EN 1993-1-4 [66].

$$\varepsilon_{ave,\theta} = 0.85\varepsilon_{ave} = 0.85\sqrt{\frac{235}{f_{y,ave}}\frac{E}{210000}} \tag{7}$$

3.2. Cross-section resistance

According to EN 1993-1-2 [1], the design cross-section axial compression resistance $N_{fi,t,Rd}$ for temperature θ at time t is determined by Eqs. (8) and (9),

$$N_{fi,t,Rd} = Ak_{2,\theta}f_y/\gamma_{M,fi} \text{ for Class 1, 2 and 3 cross-sections} \quad (8)$$

$$N_{fi,t,Rd} = A_{eff}k_{p0.2,\theta}f_y/\gamma_{M,fi} \text{ for Class 4 cross-sections} \quad (9)$$

where A and A_{eff} are the full and effective cross-section areas and $\gamma_{M,fi}$ is the partial safety factor for fire design equal to unity.

EN 1993-1-2 [1] recommends the effective cross-section properties at elevated temperatures to be taken the same as those for room temperature design. For CHS and EHS, as recommended in Chan and Gardner [26], the effective section area A_{eff} can be determined using the following equation:

$$A_{eff} = A\sqrt{\frac{90}{D_e/t}\frac{235}{f_y}} \quad (10)$$

Note that Eq. (10) will appear in the upcoming version of EN 1993-1-4 [66] for the determination of the effective cross-section areas of stainless steel CHS and EHS under pure axial compression. For SHS and RHS, the effective cross-section area A_{eff} is calculated through the effective width method provided in EN 1993-1-4 [66] by reducing the widths of the slender constituent plates through local buckling reduction factors ρ as determined by:

$$\rho = \frac{0.772}{\bar{\lambda}_p} - \frac{0.079}{\bar{\lambda}_p^2} \text{ but } \rho \leqslant 1.0 \quad (11)$$

In Eq. (11), $\bar{\lambda}_p$ is the room temperature non-dimensional plate slenderness given by:

$$\bar{\lambda}_p = \sqrt{\frac{f_y}{\sigma_{cr}}} \quad (12)$$

where σ_{cr} is the elastic local buckling stress of the plate (i.e. flange or web) determined through:

$$\sigma_{cr} = k_\sigma \frac{\pi^2 E}{12(1-\nu^2)}\left(\frac{t}{b}\right)^2 \quad (13)$$

In Eq. (13), E is the Young's modulus, υ is the Poisson's ratio equal to 0.3, t and b are the plate thickness and width of the flat regions and k_σ is the plate buckling coefficient determined in accordance with the provisions of the European design standard for plated structural elements EN 1993-1-5 [53].

As presented in Eq. (8) and (9), according to EN 1993-1-2 [1], the elevated temperature material strengths at 2% total strain $f_{2,\theta} = k_{2,\theta}f_y$ are used as the reference material strengths in the determination of the ultimate resistances of Class 1, 2 and 3 cross-sections, while the elevated temperature 0.2% proof strengths $f_{p0.2,\theta} = k_{p0.2,\theta}f_y$ are used for Class 4 cross-sections. Therefore, there is an artificial step between the design cross-section resistances of Class 3 and Class 4 cross-sections according to the provisions of EN 1993-1-2 [1].

It should be noted that, as indicated in Section 3.1, for the determination of the cross-section resistances of cold-formed SHS and RHS, the average room temperature 0.2% proof strengths of the cross-sections $f_{y,ave}$ can be used for design [41,67]. If the elevated temperature material strengths $f_{2,\theta}$ and $f_{p0.2,\theta}$ determined through $f_{y,ave}$ are adopted for the fire design of cold-formed stainless steel SHS and RHS, the room temperature 0.2% proof strengths f_y used in Eqs. (8), (9) and (12) should also be replaced with $f_{y,ave}$.

3.3. Flexural buckling resistance

EN 1993-1-2 [1] provides the same flexural buckling design rules for carbon steel and stainless steel columns in fire, despite the significantly different elevated temperature material response of stainless steel and carbon steel which considerably influence the member behaviour at elevated temperatures. The format of the elevated temperature flexural buckling design rules of EN 1993-1-2 [1] are similar to that of the room temperature flexural buckling design rules provided in EN 1993-1-1 [65], which were developed on the basis of the Perry-Robertson concept [68,69]. According to EN 1993-1-2 [1], the flexural buckling resistance $N_{b,fi,t,Rd}$ of a stainless steel column for temperature θ at time t is determined by multiplying the elevated temperature flexural buckling reduction factor χ_{fi} by the design cross-section resistance $N_{fi,t,Rd}$ (see Section 3.2), as expressed by the following formulae:

$$N_{b,fi,t,Rd} = \frac{\chi_{fi}Ak_{2,\theta}f_y}{\gamma_{M,fi}} \text{ for Class 1, 2 and 3 cross-sections} \quad (14)$$

$$N_{b,fi,t,Rd} = \frac{\chi_{fi}A_{eff}k_{p0.2,\theta}f_y}{\gamma_{M,fi}} \text{ for Class 4 cross-sections} \quad (15)$$

In Eqs. (14) and (15), the elevated temperature flexural buckling reduction factor χ_{fi} is determined through the following equation,

$$\chi_{fi} = \frac{1}{\phi_\theta + \sqrt{\phi_\theta^2 - \bar{\lambda}_\theta^2}} \text{ where } \phi_\theta = 0.5\left[1 + \eta_\theta + \bar{\lambda}_\theta^2\right] \quad (16)$$

where η_θ is the generalised imperfection factor as given by:

$$\eta_\theta = \alpha\bar{\lambda}_\theta \text{ with } \alpha = 0.65\sqrt{235/f_y} \quad (17)$$

and $\bar{\lambda}_\theta$ is the non-dimensional elevated temperature member slenderness as determined by:

$$\bar{\lambda}_\theta = \bar{\lambda}\sqrt{\frac{k_{2,\theta}}{k_{E,\theta}}} = \sqrt{\frac{Af_y}{N_{cr}}}\sqrt{\frac{k_{2,\theta}}{k_{E,\theta}}} \text{ for Class 1, 2 and 3 cross-sections} \quad (18)$$

$$\bar{\lambda}_\theta = \bar{\lambda}\sqrt{\frac{k_{p0.2,\theta}}{k_{E,\theta}}} = \sqrt{\frac{A_{eff}f_y}{N_{cr}}}\sqrt{\frac{k_{p0.2,\theta}}{k_{E,\theta}}} \text{ for Class 4 cross-sections} \quad (19)$$

In Eqs. (18) and (19), $\bar{\lambda}$ is the room temperature member slenderness and N_{cr} is the elastic critical flexural buckling load. For cold-formed stainless steel SHS and RHS, the material strength f_y may be replaced by the average material strength $f_{y,ave}$ in the determination of the design elevated temperature flexural buckling resistance $N_{b,fi,t,Rd}$. The accuracy of the fire design rules provided in EN 1993-1-2 [1] is assessed in Section 5 for a broad range of stainless steel hollow section columns.

4. Development of a new fire design method for stainless steel hollow section columns

In this section, the new proposals for the flexural buckling assessment of stainless steel CHS, EHS, SHS and RHS columns at elevated temperatures are presented. Similar to the column fire design method provided in EN 1993-1-2 [1], in the new design method developed in this study, the design resistances of stainless steel hollow section columns $N_{b,fi,t,Rd}$ are determined by multiplying the proposed flexural buckling reduction factors χ_{fi} by the design cross-section resistances $N_{fi,t,Rd}$; the design cross-section resistances $N_{fi,t,Rd}$ are calculated using the fire cross-section design methods developed in [64] and [52] for stainless steel CHS/EHS and SHS/RHS, respectively. In this section, firstly, the new cross-section classification system and cross-section design rules used to determine the cross-section resistances of stainless steel CHS/EHS and SHS/RHS at elevated temperatures developed in [52,64] are introduced in Sections 4.1 and 4.2. Then, a new set of flexural buckling

Table 6
Auxiliary factors for determination of effective section area of stainless steel CHS and EHS under compression [64].

Cross-section	Grade	η	β	φ
CHS	A	0.4	1.0	0.6
	D	0.4	1.0	0.7
	F	0.3	0.8	0.9
EHS	A	0.4	0.8	0.6
	D	0.4	0.8	0.7
	F	0.3	0.7	0.9

design curves for stainless steel hollow section columns in fire are derived in Section 4.3.

4.1. Cross-section classification

As indicated in Section 3.1, the average material strengths $f_{y,ave}$ calculated through Eq. (6) can be adopted in the cross-section classification and determination of the cross-section design resistances of cold-formed stainless steel SHS and RHS members at elevated temperatures. To achieve efficient designs, this study recommends the use of the average material strengths in the determination of the ultimate resistances of cold-formed stainless steel SHS and RHS columns in fire. For the sake of generality, the reference room temperature 0.2% proof strengths f_y* used in the proposed fire design rules in this paper in conjunction with proper reductions at elevated temperatures can be expressed by Eq. (20).

$$\begin{aligned} f_y^* &= f_{y,ave} \text{ for cold-formed SHS/RHS} \\ f_y^* &= f_y \text{ for CHS/EHS and hot-rolled SHS/RHS} \end{aligned} \tag{20}$$

Although the consideration of the strength enhancement in the corner regions is recommended herein in the determination of the resistances of cold-formed stainless steel SHS/RHS, this strength enhancement can also be conservatively neglected and only the material strength in the flat portions of the SHS/RHS can be uniformly adopted.

According to the new fire cross-section design methods developed in [52,64], all stainless steel cross-sections are classified into two classes referred to as (i) 'non-slender' and (ii) 'slender' on the basis of their cross-section slenderness or the plate slendernesses of their constituent elements at elevated temperatures $\bar{\lambda}_{p,\theta}$, replacing the four-class cross-section classification system given in EN 1993-1-4 [66] for room temperature design. This design approach is fully in accordance with the new stainless steel fire cross-section classification rules put forward in Xing et al. [70], which will be incorporated into prEN 1993-1-2 [13].

For a stainless steel CHS/EHS, when the elevated temperature cross-section slenderness $\bar{\lambda}_{p,\theta}$ is not greater than the threshold slenderness $\bar{\lambda}_{p0,\theta}$ (i.e., $\bar{\lambda}_{p,\theta} \leq \bar{\lambda}_{p0,\theta}$), the CHS/EHS is classified as a 'non-slender' cross-section. Otherwise, it is classified as a 'slender' cross-section, for which the effective cross-section properties should be used to determine the cross-section resistance in fire. The elevated temperature cross-section slenderness $\bar{\lambda}_{p,\theta}$ is determined by:

$$\bar{\lambda}_{p,\theta} = \xi_\theta \sqrt{\frac{f_y^*}{\sigma_{cr}}} \text{ with } \xi_\theta = \sqrt{\frac{k_{2,\theta}}{k_{E,\theta}}} \tag{21}$$

where ξ_θ is the elevated temperature strength-to-stiffness ratio factor and σ_{cr} is the elastic critical local buckling stress of CHS/EHS at room temperature as determined by Eq. (22) [71,72].

$$\sigma_{cr} = \frac{E}{\sqrt{3(1-\nu^2)}} \frac{2t}{D_e} \tag{22}$$

According to the design method provided in [64], the threshold slenderness $\bar{\lambda}_{p0,\theta}$ used in the cross-section classification for stainless steel CHS/EHS in fire is calculated as

$$\bar{\lambda}_{p0,\theta} = \left(\eta - 0.2\sqrt{235/f_y}\right)\sqrt{\xi_\theta} \tag{23}$$

where η is the auxiliary coefficient; the recommended values of η for austenitic, duplex and ferritic CHS and EHS under compression in fire are given in Table 6.

For stainless steel SHS and RHS, according to the design method developed in [52], the cross-section class is determined on the basis of the elevated temperature slendernesses $\bar{\lambda}_{p,\theta}$ of the constituent plate elements within the cross-sections. When the elevated temperature plate slenderness of a cross-section plate element $\bar{\lambda}_{p,\theta}$ is smaller than or equal to a plateau slenderness $\bar{\lambda}_{p0,\theta}$ (i.e., $\bar{\lambda}_{p,\theta} \leq \bar{\lambda}_{p0,\theta}$), the cross-section plate element is classified as non-slender, otherwise it is classified as slender. A SHS/RHS including at least one slender plate element is categorised as a slender cross-section. On the other hand, only if all the constituent plate elements are classified as non-slender, the SHS/RHS is classified as a non-slender cross-section. The elevated temperature plate slenderness $\bar{\lambda}_{p,\theta}$ is determined through:

$$\bar{\lambda}_{p,\theta} = \xi_\theta \sqrt{\frac{f_y^*}{\sigma_{cr}}} \text{ with } \xi_\theta = \sqrt{\frac{k_{2,\theta}}{k_{E,\theta}}} \tag{24}$$

where σ_{cr} is the elastic local buckling stress of the plate element at room temperature as determined by Eq. (13).

According to the cross-section fire design method developed in [52], the plateau slendernesses $\bar{\lambda}_{p0,\theta}$ for the cross-section elements of stainless steel SHS and RHS are calculated as:

$$\bar{\lambda}_{p0,\theta} = \begin{cases} \left(0.27 + \sqrt{0.0279 - 0.015\psi}\right)^{1.33}\sqrt{\xi_\theta} & \text{for austenitic} \\ \left(0.3 + \sqrt{0.045 - 0.015\psi}\right)^{1.33}\sqrt{\xi_\theta} & \text{for duplex and ferritic} \end{cases} \tag{25}$$

where ψ is the ratio of the normal stresses at the two edges of the plate element as defined in EN 1993-1-5 [53]; ψ is equal to 1.0 for the pure axial compression case.

4.2. Cross-section resistance

As indicated in Section 1, the adoption of $f_{2,\theta}$ and $f_{p0.2,\theta}$ as the reference material strength for different cross-section classes in the determination of the cross-section resistances results in artificial steps in the resistance predictions between difference cross-section classes and conservative resistance predictions for slender cross-sections [12]. To eliminate these shortcomings, Couto et al. [12] and prEN 1993-1-2 [13] recommended the consistent use of $f_{2,\theta}$ as the reference material strength for all cross-section classes. In line with [12,13], the new proposals in [52,64] also recommended to the consistently use $f_{2,\theta} = k_{2,\theta} f_y$* as the reference material strength for all cross-section classes to determine the ultimate cross-section resistances at elevated temperatures. Thus, this study recommends the determination of the design cross-section axial compression resistances $N_{fi,t,Rd}$ of stainless steel cross-sections for temperature θ at time t by:

$$N_{fi,t,Rd} = \frac{A k_{2,\theta} f_y^*}{\gamma_{M,fi}} \text{ for non-slender sections} \tag{26}$$

$$N_{fi,t,Rd} = \frac{A_{eff} k_{2,\theta} f_y^*}{\gamma_{M,fi}} \text{ for slender sections} \tag{27}$$

In the case of stainless steel CHS and EHS at elevated temperatures, according to the cross-section fire design method provided in [64], the effective cross-section area A_{eff} used in Eq. (27) can be calculated by:

$$A_{eff} = \rho A \tag{28}$$

In Eq. (28), ρ is the local buckling reduction factor as determined by Eq. (29) and (30) for non-slender and slender CHS/EHS respectively,

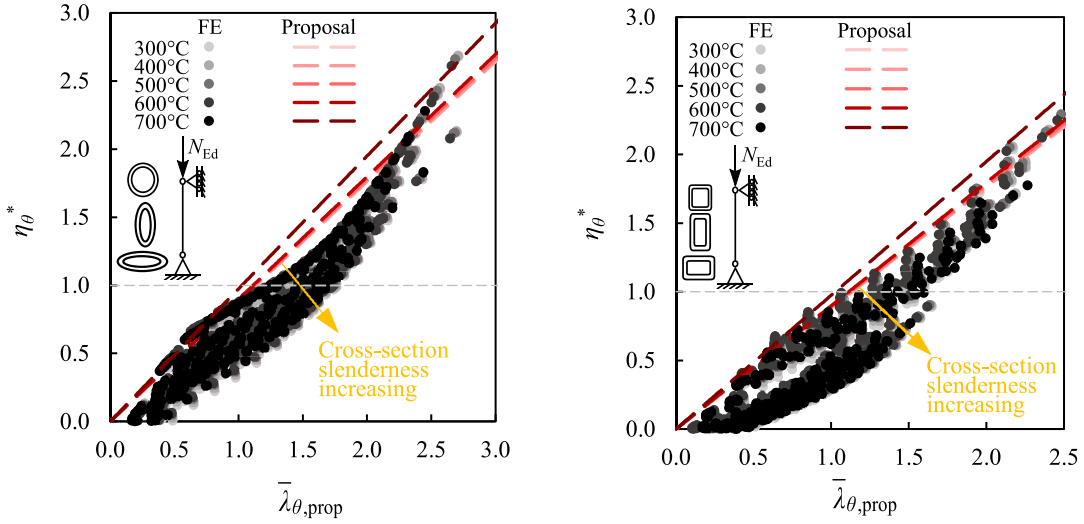

Fig. 6. Calibration of generalised imperfection factor η_θ^* for cold-formed austenitic stainless steel CHS/EHS and SHS/RHS columns.

where β and φ are the auxiliary coefficients as derived in [64] and provided in Table 6.

$$\rho = 1.0 \text{ for non-slender CHS/EHS with } \bar{\lambda}_{p,\theta} \leqslant \bar{\lambda}_{p0,\theta} \tag{29}$$

$$\rho = 1 - \beta\left(\frac{\bar{\lambda}_{p,\theta} - \bar{\lambda}_{p0,\theta}}{\sqrt{\xi_\theta}}\right)^{\varphi} \text{ for slender CHS/EHS with } \bar{\lambda}_{p,\theta} > \bar{\lambda}_{p0,\theta} \tag{30}$$

In the case of stainless steel SHS and RHS at elevated temperatures, according to the design method provided in [52], the effective cross-section area A_{eff} is determined by taking into consideration the effective widths b_{eff} of each constituent plate within the cross-section; the effective widths b_{eff} are determined by multiplying the plate widths b by the local buckling reduction factors ρ following the procedure provided in EN 1993-1-5 [53] as given by:

$$b_{eff} = \rho b \tag{31}$$

The local buckling reduction factor ρ is taken equal to 1.0 for non-slender plates as given by

$$\rho = 1.0 \text{ for } \bar{\lambda}_{p,\theta} \leqslant \bar{\lambda}_{p0,\theta} \tag{32}$$

and calculated using Eq. (33) for slender internal stainless steel plates at elevated temperatures

$$\rho = \begin{cases} \dfrac{0.54}{\left(\bar{\lambda}_{p,\theta}/\sqrt{\xi_\theta}\right)^{0.75}} - \dfrac{0.015(3+\psi)}{\left(\bar{\lambda}_{p,\theta}/\sqrt{\xi_\theta}\right)^{1.5}} \text{ for } \bar{\lambda}_{p,\theta} > \bar{\lambda}_{p0,\theta} \text{ (austenitic)} \\ \dfrac{0.6}{\left(\bar{\lambda}_{p,\theta}/\sqrt{\xi_\theta}\right)^{0.75}} - \dfrac{0.015(3+\psi)}{\left(\bar{\lambda}_{p,\theta}/\sqrt{\xi_\theta}\right)^{1.5}} \text{ for } \bar{\lambda}_{p,\theta} > \bar{\lambda}_{p0,\theta} \text{ (duplex, ferritic)} \end{cases} \tag{33}$$

in which ψ is the ratio of the normal stresses at the edges of the plate which is equal to 1.0 for the pure compression case and $\bar{\lambda}_{p0,\theta}$ is the plateau slendernesses calculated using Eq. (25).

4.3. Flexural buckling resistance

Following the methodology employed in Kucukler et al. [8] for the fire design of stainless steel I-section columns, new rules for the design of stainless steel hollow section columns at elevated temperatures are developed herein. Similar to the cross-section fire design rules provided in [52,64] and the column fire design rules provided in [8], in this study, the elevated temperature material strength at 2% total strain $f_{2,\theta} = k_{2,\theta} f_y^*$ is used as the reference material strength for the flexural buckling design of stainless steel hollow section columns in fire. The design flexural buckling resistances of stainless steel columns for temperature θ at time t can be determined using the following equations:

$$N_{b,fi,t,Rd} = \frac{\chi_{fi} A k_{2,\theta} f_y^*}{\gamma_{M,fi}} \text{ for non-slender sections} \tag{34}$$

$$N_{b,fi,t,Rd} = \frac{\chi_{fi} A_{eff} k_{2,\theta} f_y^*}{\gamma_{M,fi}} \text{ for slender sections} \tag{35}$$

in which

$$\chi_{fi} = \frac{1}{\phi_\theta + \sqrt{\phi_\theta^2 - \beta\bar{\lambda}_\theta^2}} \text{ where } \phi_\theta = 0.5\left[1 + \eta_\theta^* + \beta\bar{\lambda}_\theta^2\right] \tag{36}$$

and

$$\eta_\theta^* = \alpha\bar{\lambda}_\theta \tag{37}$$

where α is the elevated temperature imperfection factor equal to

$$\alpha = \alpha_0/\xi_\theta \tag{38}$$

In Eqs. (36) and (37), β is the auxiliary coefficient and $\bar{\lambda}_\theta$ is the non-dimensional elevated temperature column buckling slenderness as given by the following equations:

$$\bar{\lambda}_\theta = \bar{\lambda}\xi_\theta = \sqrt{\frac{A f_y^*}{N_{cr}}}\sqrt{\frac{k_{2,\theta}}{k_{E,\theta}}} \text{ for non-slender sections} \tag{39}$$

$$\bar{\lambda}_\theta = \bar{\lambda}\xi_\theta = \sqrt{\frac{A_{eff} f_y^*}{N_{cr}}}\sqrt{\frac{k_{2,\theta}}{k_{E,\theta}}} \text{ for slender sections} \tag{40}$$

The effective cross-section area A_{eff} in Eqs. (35) and (40) is calculated using the fire cross-section design rules presented in Section 4.2.

Through the ultimate flexural buckling resistances obtained from the benchmark FE models $N_{u,FE}$ for stainless steel columns at elevated temperatures, the corresponding numerical flexural buckling reduction factors χ_{FE} can be back-calculated as follows:

$$\chi_{FE} = \frac{N_{u,FE}}{A k_{2,\theta} f_y^*} \text{ for non-slender sections} \tag{41}$$

Table 7
Proposed values of imperfection factor α_0 and auxiliary coefficient β for flexural buckling design of stainless steel hollow section columns at elevated temperatures.

Type	Austenitic		Duplex		Ferritic	
	α_0	β	α_0	β	α_0	β
Cold-formed	0.85	0.70	0.60	0.85	0.50	0.85
Hot-rolled	1.15	0.70	0.75	0.85	0.65	0.85

$$\chi_{FE} = \frac{N_{u,FE}}{A_{eff} k_{2,\theta} f_y^*} \quad \text{for slender sections} \tag{42}$$

Using χ_{FE}, Eq. (36) can be expressed in terms of the numerical generalised imperfection factor $\eta_{\theta,FE}$* as below.

$$\eta_{\theta,FE}^* = \left(\frac{1}{\chi_{FE}} - 1\right)\left(1 - \beta\chi_{FE}\bar{\lambda}_\theta^2\right) \tag{43}$$

Fig. 6 shows the numerical generalised imperfection factors $\eta_{\theta,FE}$* derived for the studied cold-formed austenitic stainless steel CHS/EHS columns and SHS/RHS columns at elevated temperatures. Calibrating η_θ* given by Eq. (37) against the numerical generalised imperfection factors $\eta_{\theta,FE}$* calculated using Eq. (43), the imperfection factors α_0 and the auxiliary coefficients β used to determine the flexural buckling resistances of stainless steel hollow section columns in fire were derived in this study. The derived imperfection factors α_0 and the auxiliary coefficients β are presented in Table 7.

As can be seen from Fig. 6, the calibrated values of η_θ* given by Eq. (37) generally agree well with the numerical values of $\eta_{\theta,FE}$* for columns with non-slender cross-sections. However, with increasing cross-section slendernesses of stainless steel columns, the calibrated values of η_θ* become much higher than the numerical values of $\eta_{\theta,FE}$*, thus leading to overly-conservative flexural buckling resistances. The underestimation of the ultimate strengths of steel columns with slender cross-sections is an inherent feature of the Perry-Robertson concept [68,69] and has been previously observed for steel and stainless steel members with slender sections at room temperature and elevated temperatures [73–75]. In this study, for the consideration of the influence of local buckling on the shape of the flexural buckling curves, the use of $\sqrt{A_{eff}/A}$ is recommended in the determination of the elevated temperature imperfection factor α, as given by Eq. (44). Note that for columns with non-slender cross-sections, α is equal to α_0/ξ_θ, consistent with Eq. (38).

$$\alpha = \alpha_0 \sqrt{\frac{A_{eff}}{A}} \Big/ \xi_\theta \tag{44}$$

Fig. 7 presents comparisons of the FE results with the proposed flexural buckling curves for a number of cold-formed austenitic stainless steel EHS and RHS columns with non-slender and slender cross-sections at elevated temperatures θ = 400 °C and 600 °C. The ultimate flexural buckling resistances N_u obtained from the GMNIA are normalised by the design cross-section resistances calculated using the design method proposed in [64] $N_{cs,prop}$ (see Section 4.2). The proposed flexural buckling curves versus the corresponding member slendernesses $\bar{\lambda}_{\theta,prop}$

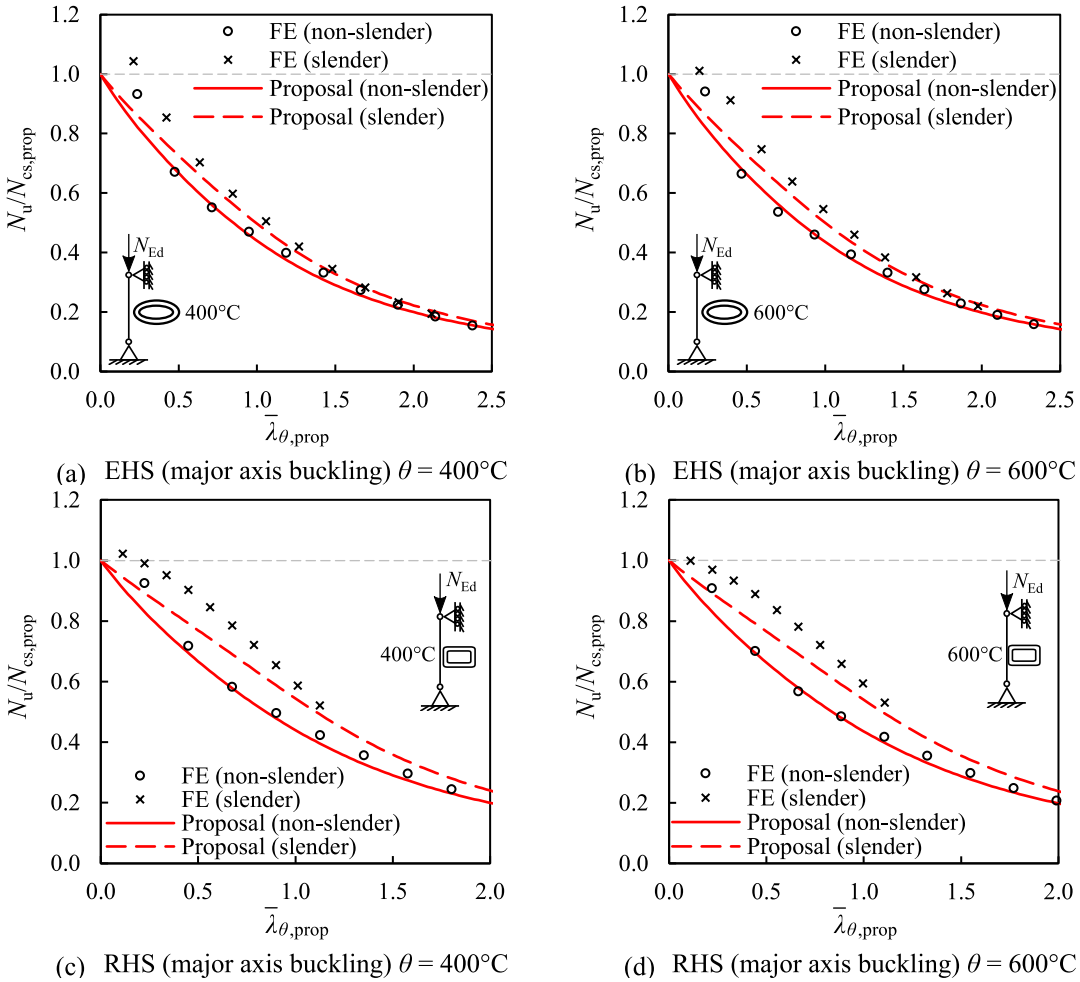

Fig. 7. Comparisons of FE results with the proposed flexural buckling curves for cold-formed austenitic stainless steel EHS and RHS columns with non-slender and slender cross-sections.

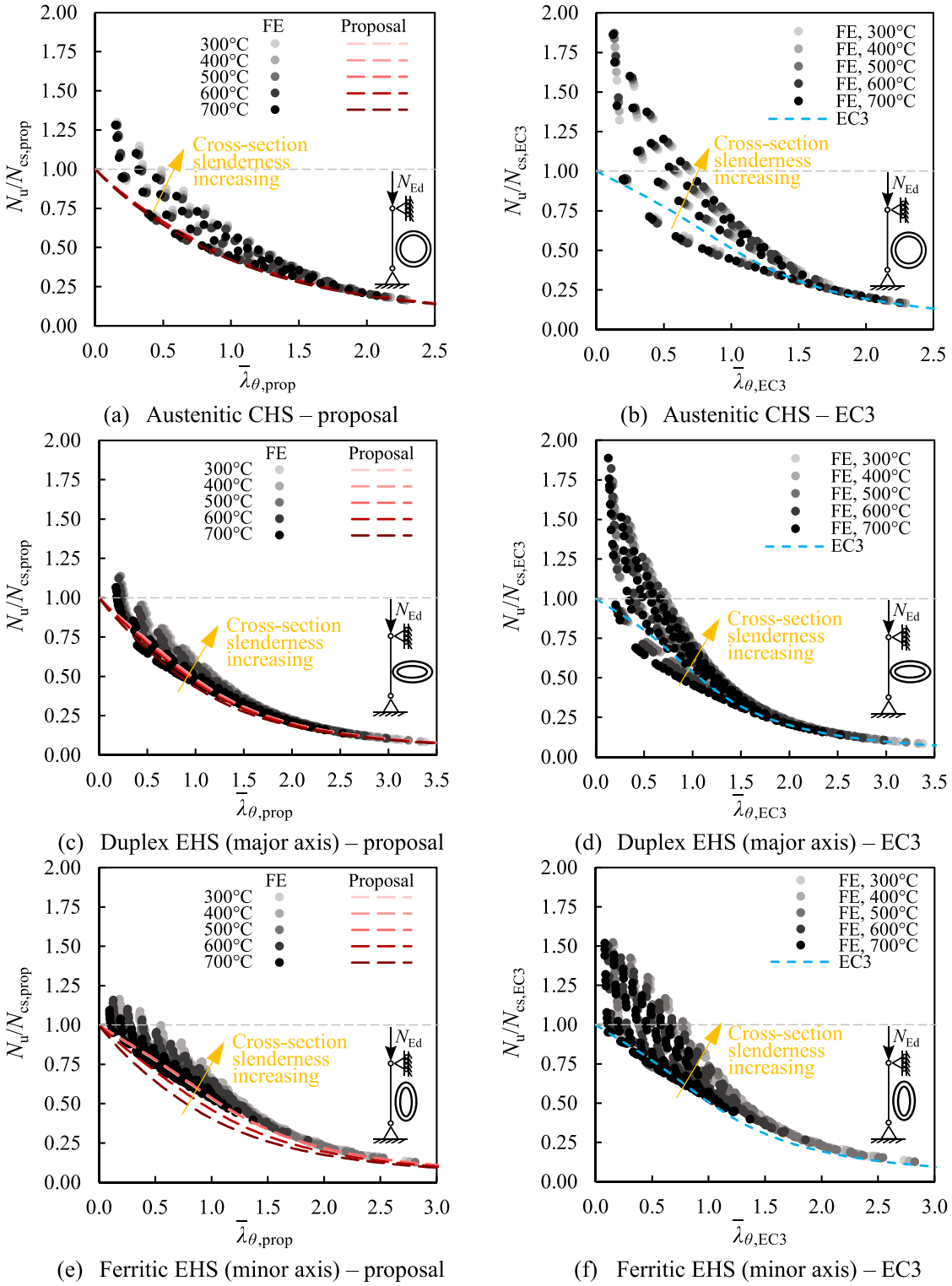

Fig. 8. Comparisons of FE results with the proposed flexural buckling curves (for non-slender cross-sections) and EN 1993-1-2 flexural buckling curve for cold-formed stainless steel CHS and EHS columns.

are also shown in Fig. 7. It can be seen from the figure that the numerical data for the columns with slender cross-sections can lie considerably above those determined for the columns with non-slender cross-sections, which was also observed in [6]. The use of the proposed imperfection factor α without considering the influence of the local buckling effects on the shapes of flexural buckling curves, as given by Eq. (38), still leads to accurate predictions for columns with non-slender cross-sections, but can result in somewhat overly-conservative predictions for columns with slender cross-sections. On the other hand, introducing $\sqrt{A_{eff}/A}$ into α, as given by Eq. (44), improves the accuracy of the resistance predictions for stainless steel columns with slender cross-sections in fire. Note that the length-to-outer diameter ratios L/D, length-to-cross-section depth ratios L/H and the length-to-cross-section width ratios L/B of the studied columns in parametric studies was up to 50 (see

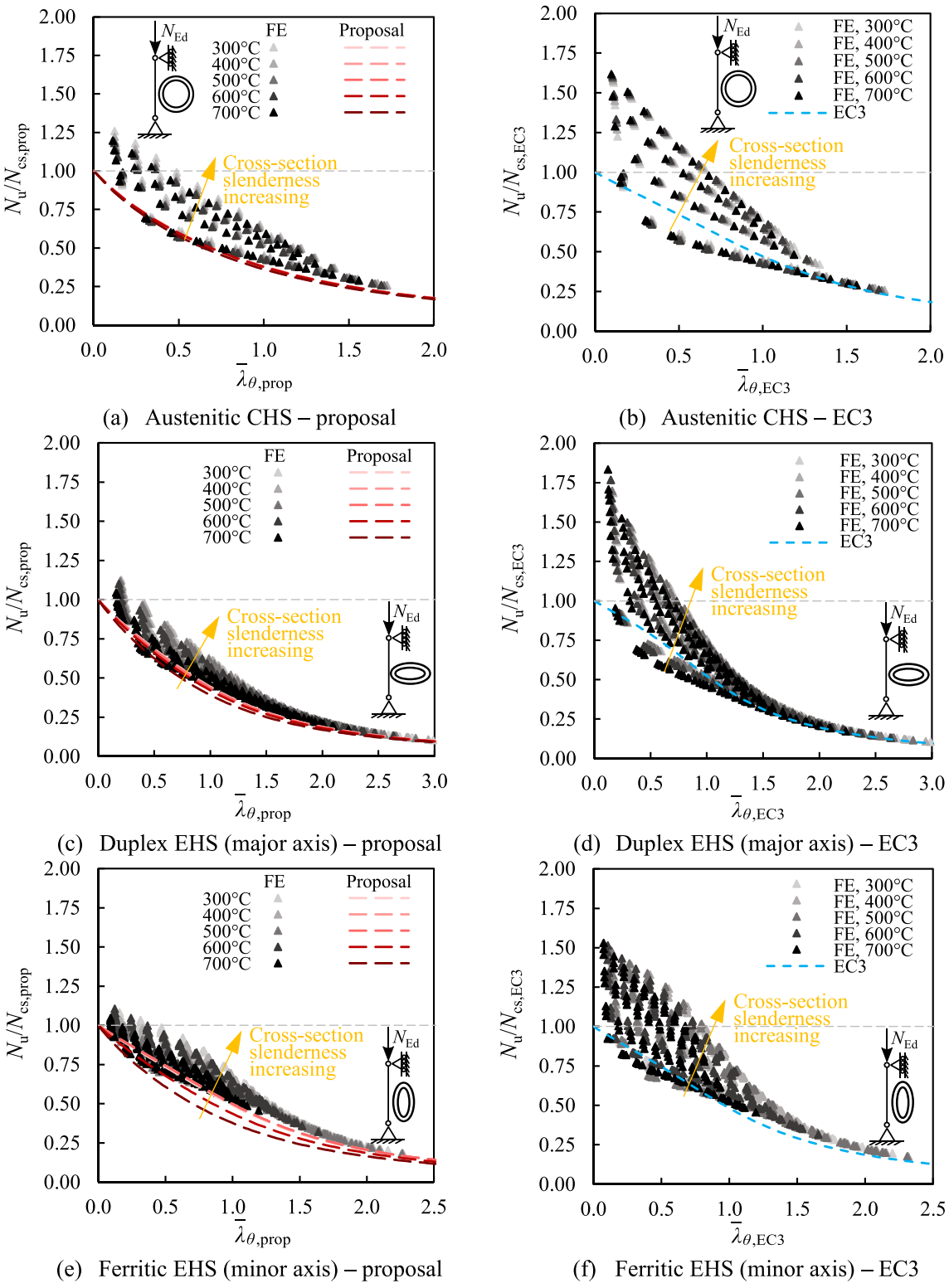

Fig. 9. Comparisons of FE results with the proposed flexural buckling curves (for non-slender cross-sections) and EN 1993-1-2 flexural buckling curve for hot-rolled stainless steel CHS and EHS columns.

Table 4) which cover the great majority of steel columns encountered in practice. However, for the extreme cases outside of this range, the use of the additional $\sqrt{A_{eff}/A}$ factor in the determination of the imperfection factor α which increases the ultimate resistances is not recommended and the imperfection factor $\alpha = \alpha_0/\xi_\theta$ as determined by Eq. (38) is conservatively employed.

5. Assessment of new elevated temperature flexural buckling design methods

In this section, the accuracy of the developed new elevated temperature flexural buckling design rules is assessed against the benchmark numerical data obtained from the shell FE models and also

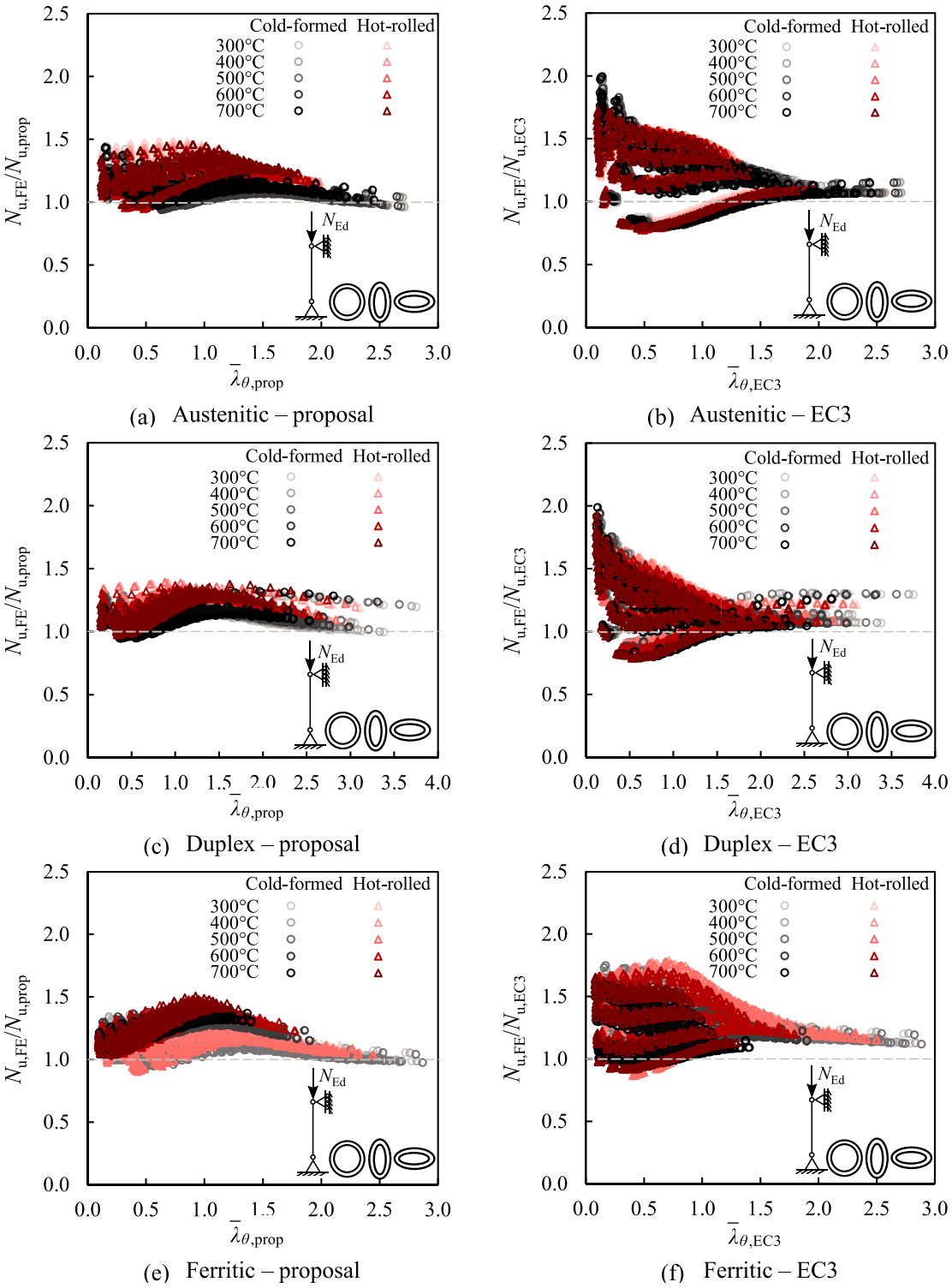

Fig. 10. Comparison of the flexural buckling resistance predictions obtained through the proposed design method $N_{u,prop}$ and the provisions of EN 1993-1-2 $N_{u,EC3}$ against those from FE modelling $N_{u,FE}$ for cold-formed and hot-rolled stainless steel CHS and EHS columns.

compared against that of the column fire design rules of EN 1993-1-2 [1] for cold-formed and hot-rolled stainless steel CHS and EHS columns (in Section 5.1) and SHS and RHS columns (in Section 5.2) at elevated temperatures.

5.1. Cold-formed and hot-rolled CHS and EHS

Figs. 8 and 9 present comparisons of the flexural buckling resistance predictions obtained using the proposed new design rules and EN 1993-1-2 [1] against the benchmark ultimate resistances from the shell FE models for a series of cold-formed and hot-rolled stainless steel CHS and EHS columns in fire. The ultimate flexural buckling resistances N_u obtained from the FE models are normalised by the design cross-section resistances calculated using the design method proposed in [64] $N_{cs,prop}$ (see Section 4.2) or by the design cross-section resistances calculated using the design rules in EN 1993-1-2 [1] $N_{cs,EC3}$ (see Section 3.2) in the

Table 8
Summary of mean, CoV, maximum and minimum values of the ratios of the resistance predictions obtained from FE modelling $N_{u,FE}$ to those determined using the new proposals $N_{u,prop}$ and provisions of EN 1993-1-2 [1] $N_{u,EC3}$ for all studied cold-formed and hot-rolled stainless steel CHS and EHS columns.

Type	Grade	No.	$N_{u,FE}/N_{u,prop}$				$N_{u,FE}/N_{u,EC3}$			
			Mean	CoV	Max	Min	Mean	CoV	Max	Min
Cold-formed	A	1750	1.08	0.062	1.45	0.94	1.19	0.197	1.99	0.79
	D	1750	1.11	0.054	1.32	0.94	1.18	0.166	1.99	0.79
	F	1750	1.17	0.088	1.40	0.94	1.25	0.139	1.75	0.95
Hot-rolled	A	1750	1.21	0.088	1.49	0.95	1.21	0.203	1.73	0.77
	D	1750	1.20	0.068	1.39	0.97	1.21	0.167	1.93	0.79
	F	1750	1.21	0.096	1.51	0.90	1.30	0.164	1.79	0.86

figures. The corresponding buckling curves proposed in this study (see Section 4.3) and the buckling curves provided in EN 1993-1-2 [1] (see Section 3.3) versus the corresponding member slendernesses $\bar{\lambda}_{\theta,prop}$ or $\bar{\lambda}_{\theta,EC3}$ are also shown. As indicated in Sections 3.3 and 4.3, since the column fire design methods proposed in this paper and those provided in EN 1993-1-2 [1] employ different cross-section classification systems and different reference material strengths (i.e. $f_{p0.2,\theta}$ and $f_{2,\theta}$), the member slendernesses determined using the proposed design rules $\bar{\lambda}_{\theta,prop}$ may be different than those determined using the provisions of EN 1993-1-2 $\bar{\lambda}_{\theta,EC3}$. Note that the elevated temperature flexural buckling curves provided in EN 1993-1-2 [1] are identical for different temperature levels, while the new flexural buckling curves proposed in this study vary for different elevated temperature levels. Due to the use of $\sqrt{A_{eff}/A}$ in the imperfection factor α, the proposed flexural buckling curves also vary for different slender cross-sections. Thus, in Figs. 8 and 9, only the proposed buckling curves for columns with non-slender cross-sections are presented.

As can be seen from Figs. 8 and 9, the ultimate flexural buckling resistances obtained from the GMNIA normalised by $N_{cs,prop}$ are less scattered than those normalised by $N_{cs,EC3}$, indicating that the cross-section design method developed in [64] for CHS/EHS in fire is more accurate relative to the cross-section design rules in EN 1993-1-2 [1]. Moreover, as displayed in Figs. 8 and 9, the new flexural buckling curves proposed in this study are generally able to more accurately estimate the flexural buckling resistances of stainless steel CHS and EHS columns at elevated temperatures relative to EN 1993-1-2 [1]. It is also worth noting that EN 1993-1-2 [1] leads to rather unsafe predictions for some stainless steel CHS and EHS columns in fire, which was also observed in [6,11], while the proposed column fire design rules lead to safe ultimate resistance predictions for the considered wide range of cases. The proposed flexural buckling curves for non-slender cross-section cases lead to quite accurate ultimate resistance estimations for non-slender cross-section columns, while they provide somewhat conservative predictions for columns with slender cross-sections. As indicated in Section 4.3, this underestimation could be reduced by incorporating $\sqrt{A_{eff}/A}$ into the imperfection factor α in the determination of column resistances which is explored in Fig. 10 and Table 8.

Fig. 10 presents the ratios of the ultimate column resistances determined through the GMNIA of the shell FE models $N_{u,FE}$ to those obtained from the proposed column fire design rules $N_{u,prop}$ (i.e. $N_{u,FE}/N_{u,prop}$) and those determined using EN 1993-1-2 [1] $N_{u,EC3}$ (i.e. $N_{u,FE}/N_{u,EC3}$) for all the investigated 10,500 cold-formed and hot-rolled stainless steel CHS and EHS columns at elevated temperatures (see Table 4). A statistical evaluation of the accuracy of the proposed column fire design rules and EN 1993-1-2 [1] is also provided in Table 8, in which the mean, CoV, maximum and minimum values of the ratios of $N_{u,FE}/N_{u,prop}$ and $N_{u,FE}/N_{u,EC3}$ for all the studied stainless steel CHS and EHS columns are set out. As can be seen from Fig. 10, relative to EN 1993-1-2 [1], the proposed new column fire design rules generally lead to more accurate resistance predictions with a much lower scatter level for all the investigated CHS and EHS columnsin fire. The consideration of $\sqrt{A_{eff}/A}$ in the determination of the imperfection factor α as given by Eq. (44) leads to more accurate ultimate resistance predictions as can be seen from Fig. 10. The statistical evaluation results summarised in Table 8 also provide similar conclusions; the mean values of the ratios $N_{u,FE}/N_{u,prop}$ are closer to 1.0 with lower CoV values relative to the corresponding ratios of $N_{u,FE}/N_{u,EC3}$.

In this study, the reliability of the proposed new column fire design rules and the EN 1993-1-2 [1] provisions is also assessed through the three reliability criteria put forward in Kruppa [76]. Criterion 1 of [76] requires the resistance predictions obtained using a design method not to exceed the benchmark FE results by more than 15%; Criterion 2 of [76] requires the proportion of the unsafe design predictions to be no more than 20%; Criterion 3 of [76] requires the design predictions being located on the safe-side on average. The reliability assessment of the proposed new column fire design rules in this paper and the provisions of EN 1993-1-2 [1] is summarised in Table 9 for all the investigated stainless steel CHS and EHS columns, where Criterion 1 refers to the percentage of the unsafe resistance predictions which are higher than the benchmark FE results by more than 15%, Criterion 2 refers to the percentage of the unsafe predictions and Criterion 3 refers to the average percentage difference between the resistance predictions obtained using the design method and the benchmark FE results. As can be seen from Table 9, the new proposals satisfy all the three reliability criteria of Kruppa [76] for all the studied CHS and EHS columns, while EN 1993-1-2 [1] violates Criterion 1 (as highlighted with '*') for some groups and also slightly violates Criterion 2 for the hot-rolled austenitic stainless

Table 9
Reliability assessment of the new proposals and provisions of EN 1993-1-2 [1] against numerical results for all studied cold-formed and hot-rolled stainless steel CHS and EHS columns.

Type	Grade	New proposals			EN 1993-1-2		
		Criterion 1 (%)	Criterion 2 (%)	Criterion 3 (%)	Criterion 1 (%)	Criterion 2 (%)	Criterion 3 (%)
Cold-formed	A	0.00	7.54	−9.44	9.83*	18.57	−12.62
	D	0.00	3.26	−9.94	3.03*	13.77	−13.23
	F	0.00	2.63	−13.65	0.00	5.66	−18.58
Hot-rolled	A	0.00	5.60	−16.43	13.26*	23.14*	−13.38
	D	0.00	1.14	−16.32	2.97*	13.60	−14.86
	F	0.00	2.23	−16.30	0.23*	9.66	−21.04

* Violated criteria.

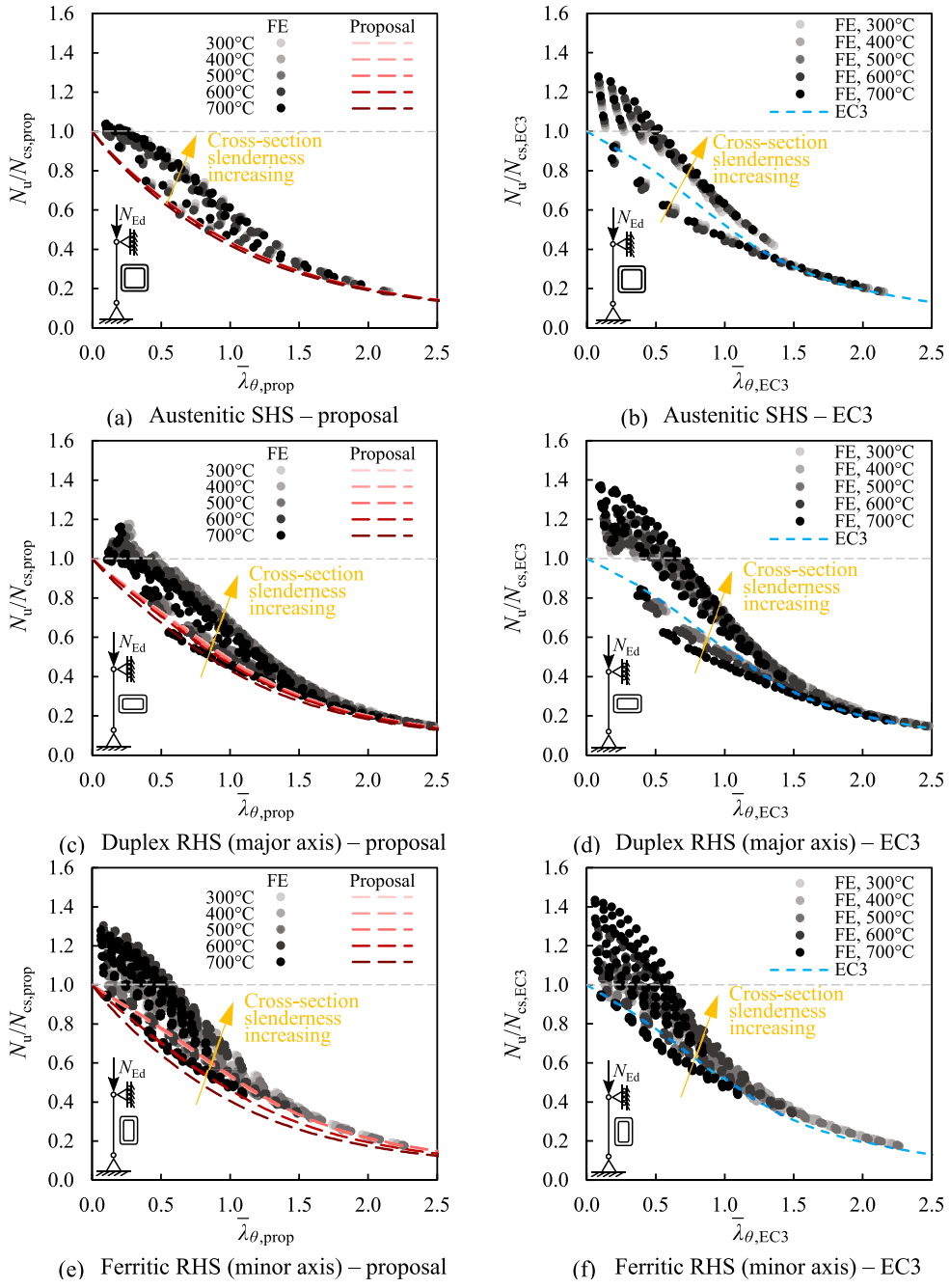

Fig. 11. Comparisons of FE results with the proposed flexural buckling curves (for non-slender cross-sections) and EN 1993-1-2 flexural buckling curve for cold-formed stainless steel SHS and RHS columns.

steel CHS and EHS columns. Considering the results presented in Table 9, it suffices to state that the new proposed column fire design rules lead to more reliable ultimate flexural buckling resistance predictions for cold-formed and hot-rolled stainless-steel CHS and EHS columns at elevated temperatures relative to EN 1993-1-2 [1].

5.2. Cold-formed and hot-rolled SHS and RHS

In this subsection, the accuracy of the proposed column fire design rules and the provisions of EN 1993-1-2 [1] is assessed for stainless steel SHS and RHS columns at elevated temperatures. Figs. 11 and 12 present the comparisons of FE results with the proposed flexural buckling curves (only for non-slender cross-sections) and EN 1993-1-2 flexural buckling curves for cold-formed and hot-rolled stainless steel SHS and RHS columns. As can be seen in Figs. 11 and 12, in line with the observations made for CHS and EHS columns, the ultimate flexural buckling resistances of SHS and RHS columns obtained from the GMNIA normalised by the cross-section resistances predicted using the method of [52] $N_{cs,prop}$ are less scattered than those normalised by the design cross-section resistances calculated using EN 1993-1-2 [1] $N_{cs,EC3}$, indicating that the cross-section design method of [52] is more accurate relative to the cross-section fire design rules of EN 1993-1-2 [1]. Figs. 11 and 12 also show that the column fire design rules proposed in this study generally lead to more accurate and consistent resistance predictions for stainless steel SHS and RHS columns in fire, while EN 1993-1-2 [1] leads to quite unsafe predictions for some cases. The resistance predictions determined using the proposed column fire design rules are particularly quite accurate for non-slender cross-section cases as can be seen from Figs. 11

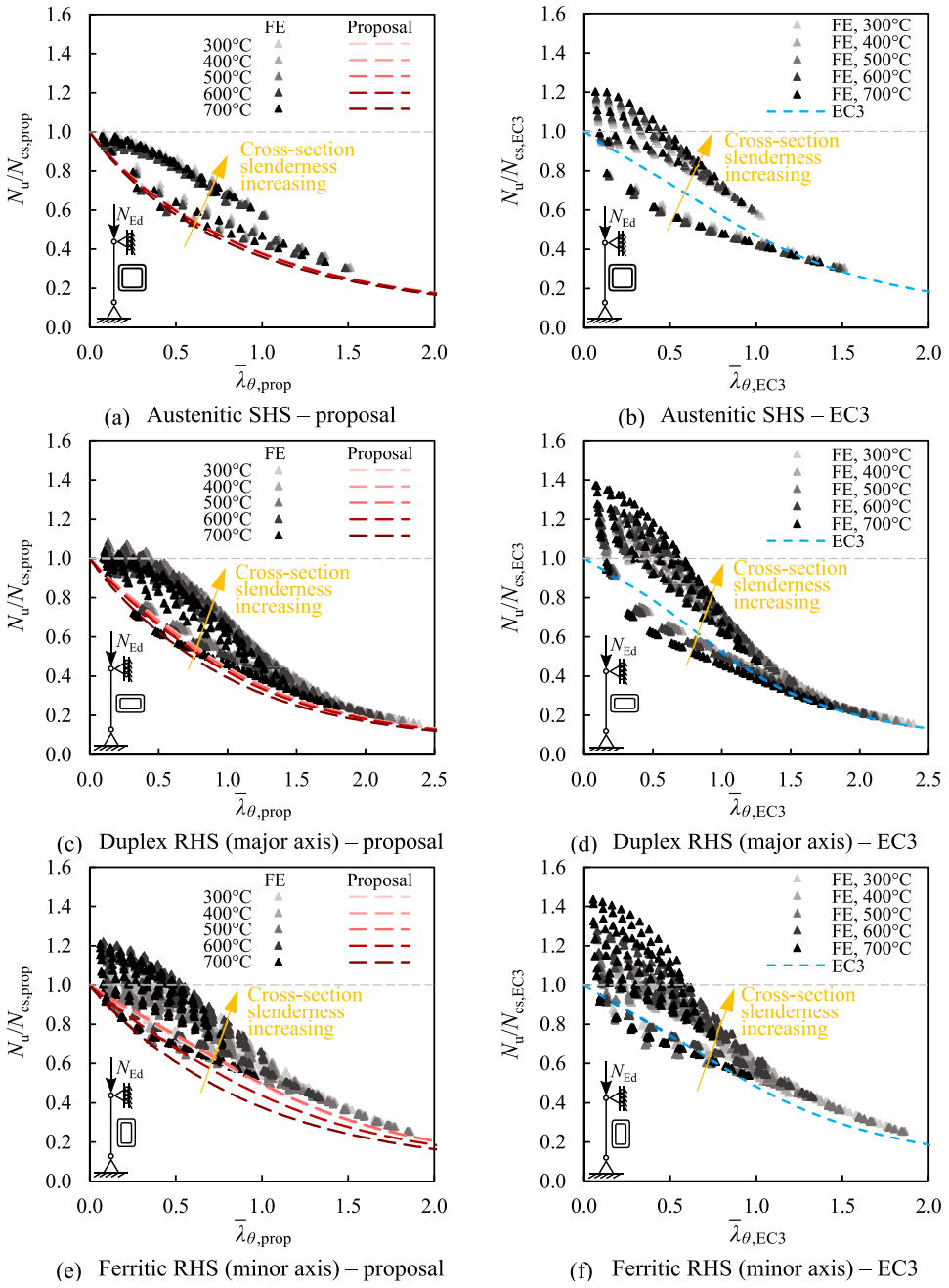

Fig. 12. Comparisons of FE results with the proposed flexural buckling curves (for non-slender cross-sections) and EN 1993-1-2 flexural buckling curve for hot-rolled stainless steel SHS and RHS columns.

and 12; the prediction accuracy for columns with slender cross-sections could be improved by the introduction of $\sqrt{A_{eff}/A}$ into the imperfection factor α, as illustrated in Fig. 7.

Fig. 13 presents the accuracy of the resistance predictions obtained using the proposed new column fire design rules $N_{u,prop}$ and provisions of EN 1993-1-2 [1]$N_{u,EC3}$ against the benchmark ultimate resistances obtained from the shell FE models $N_{u,FE}$ for all the investigated 10,500 cold-formed and hot-rolled stainless steel SHS and RHS columns at elevated temperatures (see Table 4). The statistical evaluation of the accuracy of the proposed column fire design rules and EN 1993-1-2 [1] is also illustrated in Table 10f or all the considered stainless steel SHS/RHS columns. Note that in the results presented in Fig. 13 and Table 10, the imperfection factor α is determined by Eq. (44) in the application of the proposed design rules, thereby considering the influence of $\sqrt{A_{eff}/A}$ on the shapes of the flexural buckling curves. As can be seen from Fig. 13, the design rules given in EN 1993-1-2 [1] provide quite unsafe resistance predictions for some austenitic and duplex stainless steel cases. On the other hand, the new flexural buckling design rules proposed in this study generally provide more accurate and safe resistance predictions for all the considered three material grades relative to EN 1993-1-2 [1]. As can be seen from Table 10, the CoV values of $N_{u,FE}/N_{u,prop}$ are generally smaller and the minimum values of $N_{u,FE}/N_{u,prop}$ are closer to 1.0 relative to those of $N_{u,FE}/N_{u,EC3}$, which indicate that the proposed design rules lead to both more consistent and safe ultimate resistance predictions for stainless steel SHS/RHS columns in fire relative to EN 1993-1-2 [1].

Table 11 shows the reliability assessment of the proposed design rules and the EN 1993-1-2 [1] provisions for stainless steel SHS/RHS columns at elevated temperatures using the three reliability criteria of

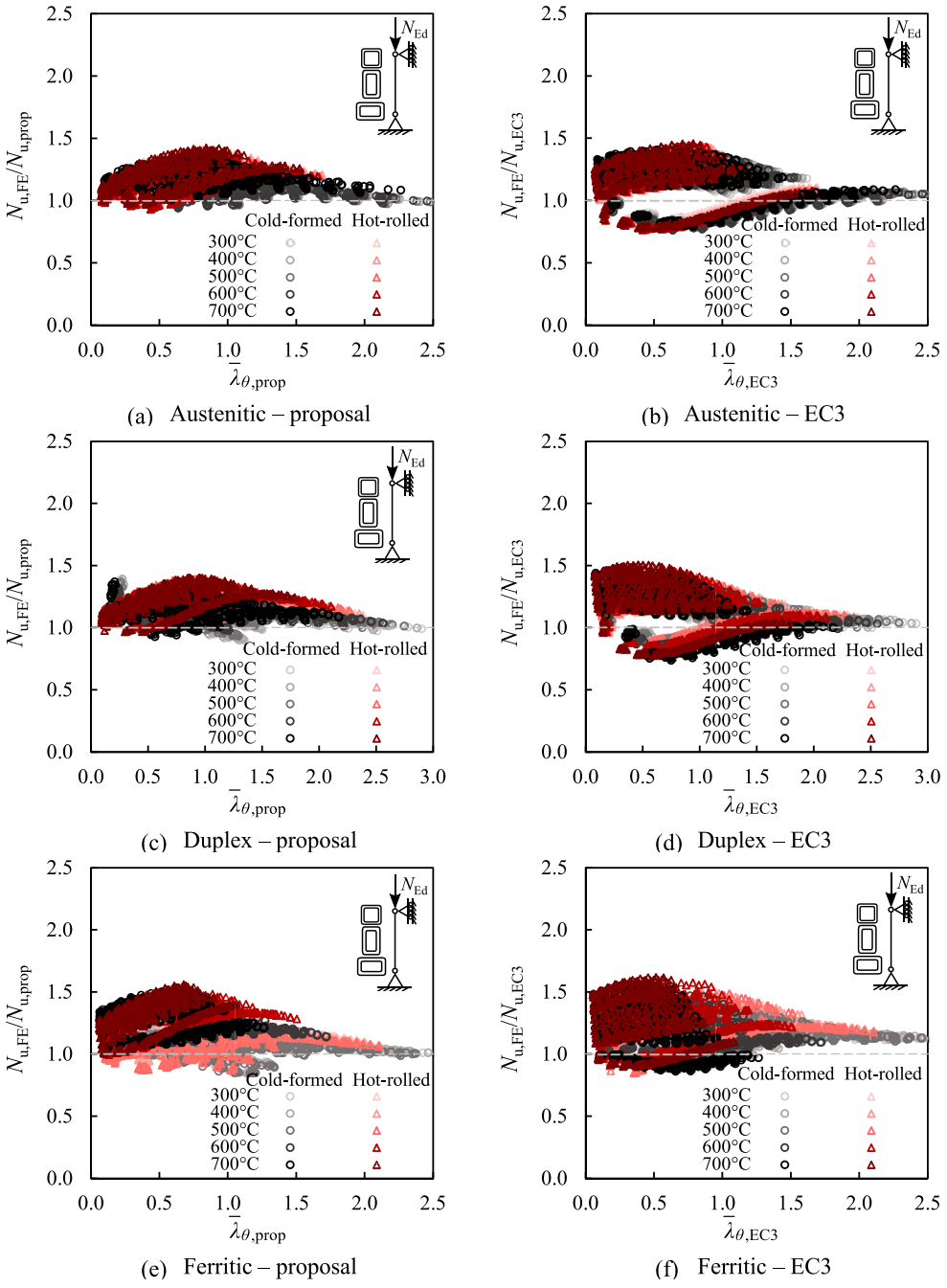

Fig. 13. Comparison of the flexural buckling resistance predictions obtained through the proposed design method $N_{u,prop}$ and the provisions of EN 1993-1-2 $N_{u,EC3}$ against those from FE modelling $N_{u,FE}$ for cold-formed and hot-rolled stainless steel SHS and RHS columns.

Table 10
Summary of mean, CoV, maximum and minimum values of the ratios of the resistance predictions obtained from FE modelling $N_{u,FE}$ to those determined using the new proposals $N_{u,prop}$ and provisions of EN 1993-1-2 [1] $N_{u,EC3}$ for all studied cold-formed and hot-rolled stainless steel SHS and RHS columns.

Type	Grade	No.	$N_{u,FE}/N_{u,prop}$				$N_{u,FE}/N_{u,EC3}$			
			Mean	CoV	Max	Min	Mean	CoV	Max	Min
Cold-formed	A	1750	1.13	0.070	1.33	0.94	1.11	0.144	1.40	0.76
	D	1750	1.12	0.070	1.39	0.90	1.13	0.131	1.48	0.74
	F	1750	1.16	0.117	1.50	0.85	1.16	0.114	1.55	0.86
Hot-rolled	A	1750	1.18	0.090	1.42	0.93	1.10	0.165	1.46	0.76
	D	1750	1.19	0.079	1.40	0.97	1.15	0.138	1.51	0.78
	F	1750	1.18	0.119	1.56	0.87	1.21	0.133	1.62	0.85

Table 11
Reliability assessment of the new proposals and provisions of EN 1993-1-2 [1] against numerical results for all studied cold-formed and hot-rolled stainless steel SHS and RHS columns.

Type	Grade	New proposals			EN 1993-1-2		
		Criterion 1 (%)	Criterion 2 (%)	Criterion 3 (%)	Criterion 1 (%)	Criterion 2 (%)	Criterion 3 (%)
Cold-formed	A	0.00	4.29	−11.05	11.09*	27.09*	−7.92
	D	0.00	5.14	−10.33	4.63*	20.29*	−9.78
	F	1.09*	7.66	−12.42	0.17*	10.46	−12.76
Hot-rolled	A	0.00	5.43	−14.49	17.26*	29.14*	−6.64
	D	0.00	1.60	−15.77	4.74*	18.80	−11.38
	F	0.00	8.86	−13.76	0.57*	13.83	−15.57

* Violated criteria.

Kruppa [76] (see Section 5.1). As can be seen from Table 11, the proposed column fire design rules only slightly violate Criterion 1 for the cold-formed ferritic stainless steel SHS/RHS columns with a very small margin of 1.09%, which is deemed to be acceptable, and satisfy all the reliability criteria for other cases. By contrast, EN 1993-1-2 [1] violates the reliability criteria of [76] for all groups. This indicates that the proposed design rules lead to more consistent and reliable ultimate flexural buckling resistance predictions for stainless-steel SHS/RHS columns at elevated temperatures relative to EN 1993-1-2 [1].

6. Consideration of different material grades

6.1. Modification of proposed column fire design rules for consideration of different stainless steel grades

In Talamona et al. [77], stability of steel columns in fire is investigated through numerical modelling where it was concluded that the yield strength has an influence on the ultimate resistances of steel columns at elevated temperatures. Based on the research performed in [77], the consideration of the material yield strength f_y is recommended in the determination of the imperfection factor as $\alpha = 0.65\sqrt{235/f_y}$ [78] in the application of the column design rules provided in EN 1993-1-2 [1] as given by Eq. (17). As indicated in Section 2.1.2, in the parametric studies performed in this paper, the standardised room temperature material properties recommended in [46] for cold-formed and hot-rolled stainless steel cross-sections were employed (see Table 1), whereby extensive shell FE data was generated. Using this extensive shell FE data on the behaviour of stainless steel hollow section columns in fire, the proposed column fire design rules was calibrated and their accuracy is comprehensively assessed and verified.

In this subsection, for the consideration of the influence of different material strengths on the flexural buckling behaviour of stainless steel columns in line with the column fire design rules of EN 1993-1-2 [1], the modification of the imperfection factor $\alpha = \alpha_0\sqrt{A_{eff}/A}/\xi_\theta$ (see Eq. (44)) derived in Section 4.3 is proposed as given by Eq. (45) in which the material factor $\sqrt{f^*_{y,st}/f^*_y}$ is introduced.

$$\alpha = \alpha_0\sqrt{\frac{A_{eff}}{A}}\sqrt{\frac{f^*_{y,st}}{f^*_y}}\Big/\xi_\theta \tag{45}$$

In Eq. (45), (i) $f^*_{y,st}$ is the standardised value of the reference room temperature 0.2% proof strength calculated by Eq. (20) using the standardised stainless steel material properties listed in Table 1 and (ii) f^*_y is the reference room temperature 0.2% proof strength also calculated by Eq. (20) using the nominal material properties of a stainless steel hollow section column. Note that for members with the standardised material properties, the material factor $\sqrt{f^*_{y,st}/f^*_y}$ is equal to 1.0, thus Eq. (45) is consistent with Eq. (44) for the columns with the standardised material properties. Using Eq. (45) to replace Eq. (44), the new design rules proposed in Section 4 can be applied to stainless steel hollow section columns with various different grades.

Table 12
Nominal material properties given in the stainless steel design standard EN 1993-1-4 [66] and Steel Construction Institute (SCI) Design Manual for Structural Stainless Steel [41] for common structural cold-formed stainless steel.

Type	Grade	Young's modulus E (N/mm^2)	Yield (0.2% proof) stress f_y (N/mm^2)	Ultimate stress f_u (N/mm^2)	Strain hardening exponent n
A I	1.4301	200,000	230	540	6
A I	1.4307		220	520	6
A II	1.4401		240	530	7
A II	1.4541		220	520	6
A III	1.4571		240	540	7
D I	1.4062	200,000	530	700	8
D I	1.4362		450	650	5
D II	1.4462		500	700	5
D II	1.4662		550	750	8
F I	1.4521	200,000	300	420	14
F I	1.4621		230	400	14
F II	1.4003		280	450	7
F II	1.4016		260	450	6

6.2. Accuracy assessment

To verify the applicability of the proposed fire design method to stainless steel columns with different material properties, in this section, a number of stainless steel columns with the nominal material properties provided in EN 1993-1-4 [66] and Steel Construction Institute (SCI) Design Manual for Structural Stainless Steel [41] were investigated. For

Table 13
Nominal material properties given in the stainless steel design standard EN 1993-1-4 [66] and Steel Construction Institute (SCI) Design Manual for Structural Stainless Steel [41] for common structural hot-rolled stainless steel.

Type	Grade	Young's modulus E (N/mm^2)	Yield (0.2% proof) stress f_y (N/mm^2)	Ultimate stress f_u (N/mm^2)	Strain hardening exponent n
A I	1.4301	200,000	210	520	6
A I	1.4307		200	520	6
A II	1.4401		220	530	7
A II	1.4541		200	520	6
A III	1.4571		220	540	7
D I	1.4062	200,000	480	680	8
D I	1.4362		400	650	5
D II	1.4462		460	700	5
D II	1.4662		550	750	8
F I	1.4521	200,000	280	400	14
F I	1.4621		230	400	14
F II	1.4003		280	450	7
F II	1.4016		240	450	6

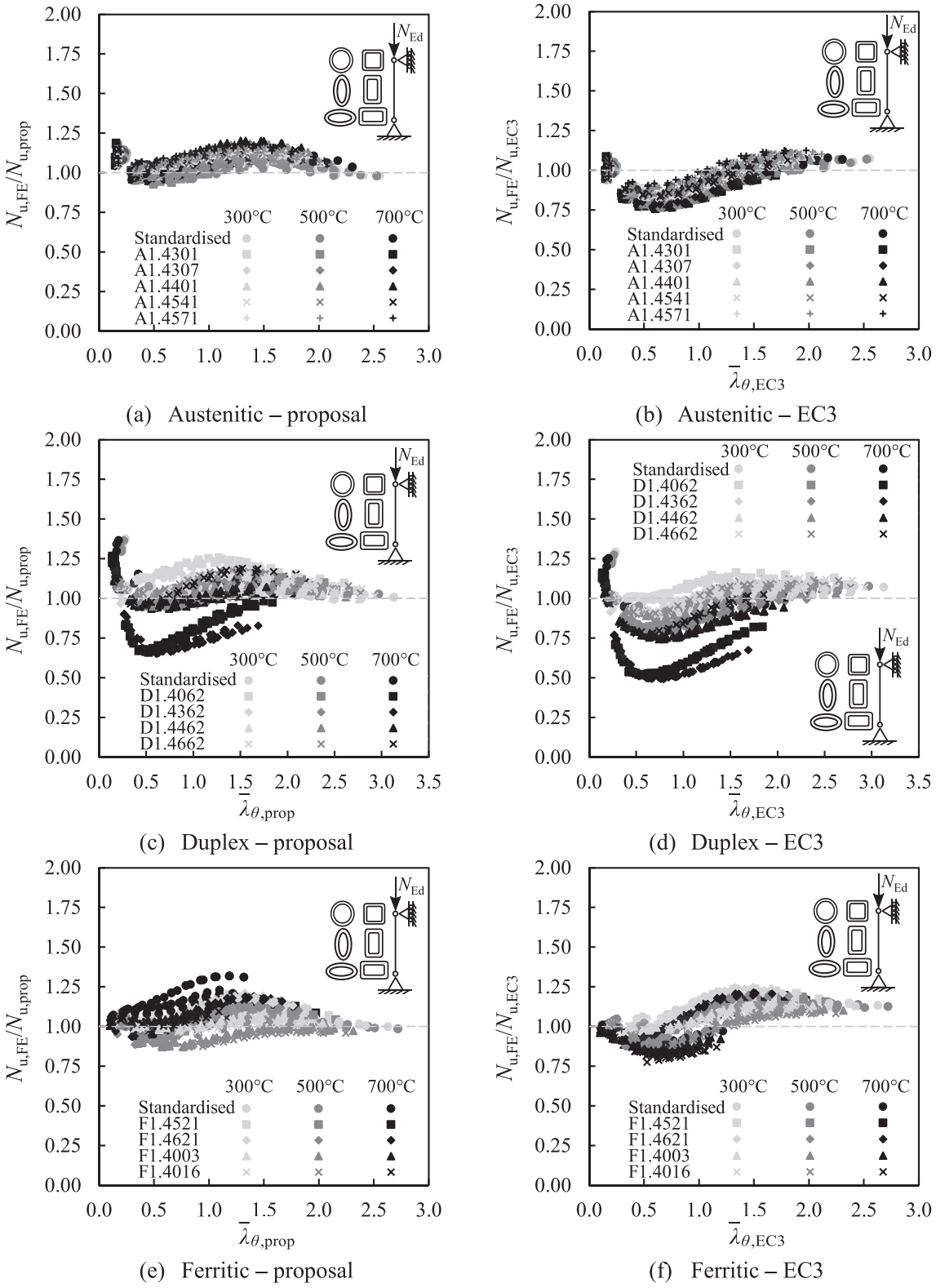

Fig. 14. Comparison of the flexural buckling resistance predictions obtained through the proposed design method $N_{u,prop}$ and the provisions of EN 1993-1-2 $N_{u,EC3}$ against those from FE modelling $N_{u,FE}$ for cold-formed stainless steel CHS, EHS, SHS and RHS columns with standardised [46] and nominal [41,66] material properties for different austenitic, duplex and ferritic stainless steel grades.

the fire design of stainless steel members, the use of different groups (i.e. I, II and III) for austenitic, duplex and ferritic stainless steel is recommended in this study in line with the grouping method of different stainless steel grades recommended in [41]; the use of the corresponding strength ($k_{p0.2,\theta}$, $k_{2,\theta}$, $k_{u,\theta}$), ductility ($k_{\varepsilon u,\theta}$) and stiffness ($k_{E,\theta}$) reduction factors provided in [41] for different stainless steel groups is recommended in the application of the proposed column fire design rules. As shown in Eq. (45), according the proposals made herein, a lower material strength f_y^* leads to a higher imperfection factor α, thereby a more

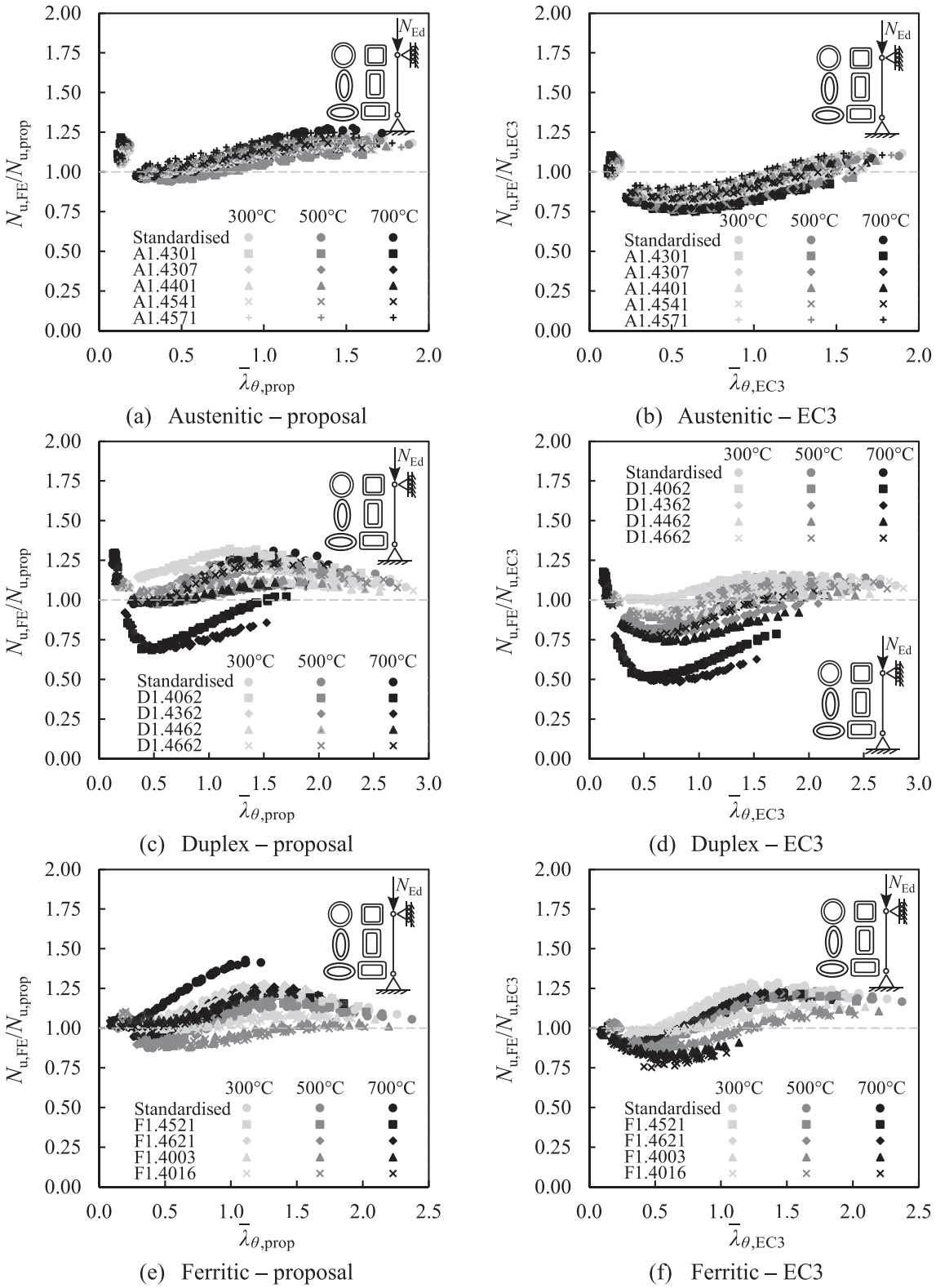

Fig. 15. Comparison of the flexural buckling resistance predictions obtained through the proposed design method $N_{u,prop}$ and the provisions given in EN 1993-1-2 $N_{u,EC3}$ against those from FE modelling $N_{u,FE}$ for hot-rolled stainless steel CHS, EHS, SHS and RHS columns with standardised [46] and nominal [41,66] material properties for different austenitic, duplex and ferritic stainless steel grades.

critical case.

A number of different stainless steel grades given in EN 1993-1-4 [66] and Steel Construction Institute (SCI) Design Manual for Structural Stainless Steel [41], including the material grades with the lowest yield strengths (i.e. 0.2% proof strengths) for each group, are adopted herein. The nominal yield strength f_y, ultimate strength f_u and strain hardening exponent n of the considered stainless steel grades are listed in Tables 12 and 13 for cold-formed and hot-rolled stainless steel columns, respectively. Note that the material properties listed in Table 12 for cold-formed stainless steel columns are the basic nominal material

Table 14
Summary of mean, CoV, maximum and minimum values of the ratios of the resistance predictions obtained from FE modelling $N_{u,FE}$ to those determined using the new proposals $N_{u,prop}$ and provisions of EN 1993-1-2 [1] $N_{u,EC3}$ for studied cold-formed stainless steel CHS, EHS, SHS and RHS columns with standardised [46] and nominal [41,66] material properties.

Type	Grade	No.	$N_{u,FE}/N_{u,prop}$				$N_{u,FE}/N_{u,EC3}$			
			Mean	CoV	Max	Min	Mean	CoV	Max	Min
A I	Standardised	180	1.05	0.044	1.15	0.94	0.96	0.094	1.08	0.78
A I	1.4301	180	1.06	0.053	1.19	0.93	0.89	0.094	1.09	0.76
A I	1.4307	180	1.05	0.055	1.16	0.93	0.88	0.094	1.06	0.76
A II	1.4401	180	1.10	0.053	1.20	0.97	0.96	0.091	1.09	0.83
A II	1.4541	180	1.08	0.046	1.17	0.98	0.93	0.082	1.07	0.82
A III	1.4571	180	1.10	0.037	1.18	1.00	1.00	0.081	1.13	0.88
D II	Standardised	180	1.10	0.037	1.18	1.00	1.00	0.081	1.13	0.88
D I	1.4062	180	1.03	0.162	1.27	0.66	0.91	0.227	1.16	0.51
D I	1.4362	180	0.97	0.169	1.23	0.65	0.85	0.237	1.12	0.49
D II	1.4462	180	1.03	0.036	1.13	0.93	0.93	0.096	1.07	0.74
D II	1.4662	180	1.09	0.055	1.19	0.94	0.99	0.098	1.13	0.77
F II	Standardised	180	1.08	0.080	1.32	0.93	1.06	0.085	1.22	0.87
F I	1.4521	180	1.07	0.071	1.18	0.89	1.09	0.101	1.24	0.88
F I	1.4621	180	1.08	0.080	1.21	0.88	1.08	0.108	1.25	0.87
F II	1.4003	180	1.01	0.054	1.15	0.87	0.99	0.100	1.15	0.83
F II	1.4016	180	1.00	0.050	1.09	0.87	0.97	0.101	1.13	0.78

properties. To account for the benefit of the strength enhancement in cold-formed stainless steel columns, enhanced material properties determined using the basic nominal material properties were used in the shell FE analyses and application of the proposed column fire design rules herein. In line with the adoption in [46], the formulae provided in Annex B of the Steel Construction Institute (SCI) Design Manual for Structural Stainless Steel [41] were utilised to calculate the enhanced material strengths of cold-formed stainless steel columns. These formulae will be incorporated into the upcoming version of EN 1993-1-4 [66]. Since there are no equations specifically provided for the determination of the enhanced material strengths of cold-formed stainless steel EHS in [41], the formulae recommended for cold-formed stainless steel CHS were also used for EHS. Note that the standardised material properties provided in [46] for cold-formed stainless steel CHS, EHS, RHS and EHS were proposed on the basis of the database from material tests on coupons extracted from cold-formed stainless steel sections. Thus, the standardised material properties listed in Table 1 could be directly used in the analysis and application of the proposed column fire design rules and the additional calculation for the strength enhancement is not required.

In the assessment of the proposed fire design rules for stainless steel hollow section columns, one CHS, EHS, SHS and RHS shape was studied for the each considered grade. For the CHS columns, $(D/t)(f_y/235)$ was taken as 20; for the EHS columns, D/B was taken as 2 and $(D_e/t)(f_y/235)$ was taken as 40. For the SHS columns, $\bar{\lambda}_{p,H}$ was taken as 0.25; for the RHS columns, H/B was taken as 1.67 and $\bar{\lambda}_{p,H}$ was taken as 0.25. The adopted cross-sections fall into the Class 1 or 2 category according to the cross-section design rules of EN 1993-1-4 [66] and the non-slender category according to the new cross-section fire design methods developed in [52,64]. For the CHS columns and EHS columns undergoing major axis flexural buckling, the length to larger outer diameter L/D ratios were ranged between 5 and 50 with an increment of 5, while for the EHS columns undergoing minor axis flexural buckling, the length to smaller diameter ratios L/B were varied from 5 to 50 with an increment of 5. Similarly, for the SHS columns and RHS columns undergoing major axis flexural buckling, the length to cross-section depth ratios L/H were varied from 5 to 50 with an increment of 5, while for the RHS columns undergoing minor axis flexural buckling, the length to cross-section width ratios L/B were ranged from 5 to 50 with an increment of 5. Three elevated temperature levels were considered: 300 °C, 500 °C and 700 °C.

Figs. 14 and 15 present comparisons of the flexural buckling

Table 15
Summary of mean, CoV, maximum and minimum values of the ratios of the resistance predictions obtained from FE modelling $N_{u,FE}$ to those determined using the new proposals $N_{u,prop}$ and the provisions in EN 1993-1-2 [1] $N_{u,EC3}$ for studied hot-rolled stainless steel CHS, EHS, SHS and RHS columns with standardised [46] and nominal [41,66] material properties.

Type	Grade	No.	$N_{u,FE}/N_{u,prop}$				$N_{u,FE}/N_{u,EC3}$			
			Mean	CoV	Max	Min	Mean	CoV	Max	Min
A I	Standardised	180	1.13	0.085	1.27	0.94	0.94	0.112	1.13	0.78
A I	1.4301	180	1.06	0.061	1.22	0.94	0.86	0.095	1.10	0.75
A I	1.4307	180	1.05	0.061	1.19	0.94	0.85	0.094	1.08	0.75
A II	1.4401	180	1.11	0.066	1.22	0.98	0.93	0.089	1.11	0.82
A II	1.4541	180	1.08	0.054	1.18	0.98	0.90	0.079	1.08	0.81
A III	1.4571	180	1.14	0.059	1.25	1.01	0.98	0.081	1.12	0.87
D II	Standardised	180	1.16	0.072	1.31	0.97	1.00	0.104	1.16	0.78
D I	1.4062	180	1.07	0.170	1.32	0.69	0.90	0.237	1.18	0.51
D I	1.4362	180	1.01	0.175	1.25	0.69	0.83	0.247	1.12	0.48
D II	1.4462	180	1.08	0.036	1.16	0.98	0.92	0.100	1.06	0.74
D II	1.4662	180	1.14	0.061	1.24	0.98	0.99	0.101	1.13	0.78
F II	Standardised	180	1.13	0.106	1.43	0.87	1.08	0.114	1.29	0.87
F I	1.4521	180	1.10	0.083	1.25	0.90	1.08	0.105	1.25	0.88
F I	1.4621	180	1.11	0.093	1.28	0.90	1.08	0.111	1.26	0.87
F II	1.4003	180	1.03	0.057	1.17	0.88	0.98	0.105	1.16	0.80
F II	1.4016	180	1.01	0.053	1.12	0.88	0.95	0.107	1.13	0.75

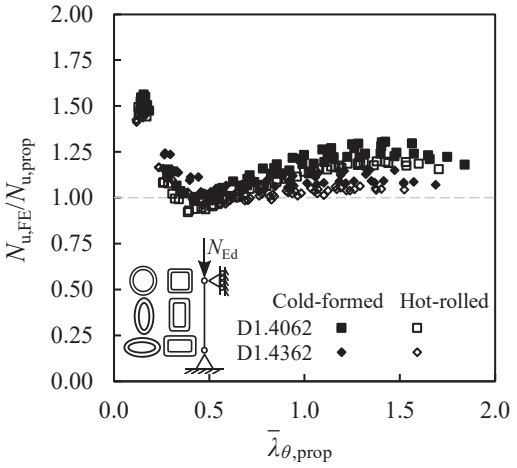

Fig. 16. Comparison of the flexural buckling resistance predictions obtained through the proposed design method $N_{u,prop}$ using the specific imperfection factor $\alpha_0 = 1.6$ and auxiliary coefficient $\beta = 0.1$ against those obtained from FE modelling $N_{u,FE}$ for cold-formed and hot-rolled duplex 1.4062 and 1.4362 stainless steel CHS, EHS, SHS and RHS columns at 700 °C.

resistance predictions obtained through the proposed design method $N_{u,prop}$ and the provisions given in EN 1993-1-2 [1] $N_{u,EC3}$ against those from shell FE models $N_{u,FE}$ for cold-formed and hot-rolled stainless steel CHS, EHS, SHS and RHS columns with standardised and nominal material properties. It can be seen from Figs. 14 and 15 that for both cold-formed and hot-rolled stainless steel hollow section columns in fire, the proposed column fire design rules generally provide accurate and safe ultimate member resistances with the exception of the columns made of duplex stainless steel grades of 1.4062 and 1.4362 at the elevated temperature level of 700 °C. On the other hand, EN 1993-1-2 [1] leads to unsafe resistance estimations almost for all the material grades. Tables 14 and 15 provide the statistical evaluation results of $N_{u,FE}/N_{u,prop}$ and $N_{u,FE}/N_{u,EC3}$ for all the studied 5760 cold-formed and hot-rolled stainless steel CHS, EHS, SHS and RHS columns with the standardised and nominal material properties, including the mean, CoV, maximum and minimum values. As can be seen from Tables 14 and 15, the mean values of the ratios $N_{u,FE}/N_{u,prop}$ are generally closer to 1.0 with lower CoV values relative to the corresponding ratios of $N_{u,FE}/N_{u,EC3}$. The accuracy improvement obtained from the proposed design method is about 10% and 13% on average for cold-formed and hot-rolled stainless steel columns, respectively, thus indicating the higher level of accuracy of the proposed fire design rules for CHS, EHS, SHS and EHS columns made of different stainless steel grades in fire.

It can be seen from Figs. 14 and 15 and Tables 14 and 15 that only for the stainless steel columns made of grade 1.4062 and 1.4362 duplex stainless steel at 700 °C, the new flexural buckling curves proposed in this study lead to rather unsafe results. These two grades fall into the Group I Duplex stainless steel category according to the Steel Construction Institute (SCI) Design Manual for Structural Stainless Steel [41]. Due to the sharp changes in the elevated temperature material reduction factors at 700 °C relative to those for lower elevated temperature levels as provided in [41], the columns made of grade 1.4062 and 1.4362 duplex stainless steel exhibit different flexural buckling behaviour at 700 °C; thus, the ultimate resistances predicted by the proposed column fire design rules become rather unsafe at 700 °C. To achieve safe design resistances for columns made of grade 1.4062 and 1.4362 duplex stainless steel, the adoption of a specific imperfection factor $\alpha_0 = 1.6$ and auxiliary coefficient $\beta = 0.1$ is proposed in the implementation of the proposed column fire design rules. Fig. 16 presents comparisons of the resistance predictions for columns made of grade 1.4062 and 1.4362 duplex stainless steel at 700 °C obtained through the GMNIA and those determined through the proposed design method but with the use of a modified imperfection factor $\alpha_0 = 1.6$ in Eq. (45) and the auxiliary coefficient $\beta = 0.1$. It can be seen from Fig. 16 that for both cold-formed and hot-rolled stainless steel columns made of grade 1.4062 and 1.4362 duplex stainless steel, the use of the modified imperfection factor $\alpha_0 = 1.6$ and auxiliary coefficient $\beta = 0.1$ moves the unsafe results to the safe side. On the basis of these observations, the use of the modified imperfection factor $\alpha_0 = 1.6$ and auxiliary coefficient $\beta = 0.1$ is recommended in the implementation of the proposed column fire design rules to stainless steel hollow section columns made of grade 1.4062 and 1.4362 duplex stainless steel.

7. Conclusions

This study investigated the flexural buckling behaviour and design of stainless steel hollow section columns at elevated temperatures. Shell FE models of stainless steel hollow section columns were created and validated against the experimental results from the literature. Following their validation, the developed shell FE models were used to carry out comprehensive numerical parametric studies to generate extensive benchmark structural performance for stainless steel hollow section columns in fire. The parametric studies took into account both cold-formed and hot-rolled austenitic, duplex and ferritic stainless steel grades, various cross-section properties, cross-section slendernesses and member slendernesses as well as different elevated temperatures levels. In the numerical parametric studies, the standardised room temperature material properties recommended in [46] were employed. In total, 21,000 stainless steel hollow section columns were taken into consideration in the numerical parametric studies, including 10,500 stainless steel CHS/EHS columns and 10,500 stainless steel SHS/RHS columns. In addition to 21,000 stainless steel columns with the standardised room temperature material properties recommended in [46], the structural response of 5760 cold-formed and hot-rolled stainless steel columns with the nominal material properties provided in EN 1993-1-4 [66] and Steel Construction Institute (SCI) Design Manual for Structural Stainless Steel [41] were also investigated, thereby considering the influence of the material strengths on the flexural buckling behaviour of stainless steel hollow section columns at elevated temperatures. Calibrated against the benchmark shell FE resistance predictions, new flexural buckling design rules for stainless steel hollow section columns at elevated temperatures were developed, which consistently consider $f_{2,\theta}$ as the reference material strength for all classes of cross-sections, in line with the recommendations in prEN1993-1-2 [13]. The accuracy of the proposed new column fire design rules is assessed for all the considered cases and also compared against the EN 1993-1-2 [1] design provisions. It was observed that the proposed new column fire design rules generally lead to more accurate and safe ultimate resistance predictions relative to the column design provisions of EN 1993-1-2 [1]. The reliability of the proposed column fire design rules and EN 1993-1-2 [1] was also assessed through the three fire reliability criteria put forward in Kruppa [76]. It was shown that for all the considered wide range of cases, the proposed new column fire design rules fulfil all the three reliability criteria of Kruppa [76]. On the other hand, it was observed that EN 1993-1-2 [1] violated the reliability criteria of [76] almost for all the considered stainless steel grades, indicating that the proposed column fire design rules provide more reliable resistance predictions relative to EN 1993-1-2 for stainless steel hollow section columns in fire.

CRediT authorship contribution statement

Chunyan Quan: Methodology, Software, Validation, Formal analysis, Investigation, Data curation, Writing – original draft, Visualization. **Merih Kucukler:** Conceptualization, Investigation, Writing – original draft, Writing – review & editing, Supervision, Project administration, Funding acquisition.

Declaration of Competing Interest

The authors declare that they have no known competing financial interests or personal relationships that could have appeared to influence the work reported in this paper.

Data availability

Data will be made available on request.

Acknowledgements

The research presented in this paper is funded by the Engineering and Physical Sciences Research Council (EPSRC) of the UK under the grant number EP/V034405/1. The authors gratefully acknowledge the financial support provided by the EPSRC for the research presented in this paper.

References

[1] EN 1993-1-2. Eurocode 3: design of steel structures-Part 1-2: general rules – structural fire design. Brussels: European Committee for Standardization; 2005.
[2] Gardner L. Stainless steel structures in fire. Proc Inst Civ Eng: Struct Build 2007; 160:129–38.
[3] N. Lopes, P. Vila Real, Fire resistance of stainless steel structural elements with class 4 square hollow sections subject to combined bending and axial compression. In: Proceedings of 8th international conference on structures in fire (SiF14 – Shanghai, 11-13/6, 2014). p. 729–36.
[4] Ng KT, Gardner L. Buckling of stainless steel columns and beams in fire. Eng Struct 2007;29:717–30.
[5] Arrais F, Lopes N, Vila Real P. Numerical study of fire resistance of stainless steel circular hollow section columns. J Fire Sci 2020;38:156–72.
[6] Arrais F, Lopes N, Vila Real P. Design of stainless steel elliptical hollow sections columns in case of fire: parametric study. Ce/Papers 2021;4:1437–46.
[7] Lopes N, Vila Real P, da Silva L, Franssen JM. Axially loaded stainless steel columns in case of fire. J Struct Fire Eng 2010;1(1):43–60.
[8] Kucukler M, Xing Z, Gardner L. Behaviour and design of stainless steel I-section columns in fire. J Constr Steel Res 2020;165:105890.
[9] Fan S, Ding X, Sun W, Zhang L, Liu M. Experimental investigation on fire resistance of stainless steel columns with square hollow section. Thin-Walled Struct 2016;98: 196–211.
[10] Fan S, Zhang L, Sun W, Ding X, Liu M. Numerical investigation on fire resistance of stainless steel columns with square hollow section under axial compression. Thin-Walled Struct 2016;98:185–95.
[11] Mohammed A, Afshan S. Numerical modelling and fire design of stainless steel hollow section columns. Thin-Walled Struct 2019;144:106243.
[12] Couto C, Vila Real P, Lopes N, Zhao B. Resistance of steel cross-sections with local buckling at elevated temperatures. J Constr Steel Res 2015;109:101–14.
[13] prEN 1993-1-2. Eurocode 3: design of steel structures – part 1-2: general rules – structural fire design; 2021.
[14] Martins AD, Gonçalves R, Camotim D. Numerical simulation and design of stainless steel columns under fire conditions. Eng Struct 2021;229.
[15] Yi S, Chen MT, Young B. Design of concrete-filled cold-formed steel elliptical stub columns. Eng Struct 2023;276:115269.
[16] Chen MT, Young B. Beam-column tests of cold-formed steel elliptical hollow sections. Eng Struct 2020;210:109911.
[17] Chen MT, Young B. Numerical analysis and design of cold-formed steel elliptical hollow sections under combined compression and bending. Eng Struct 2021;241: 112417.
[18] Chen MT, Chen Y, Young B. Experimental investigation on cold-formed steel elliptical hollow section T-joints. Eng Struct 2023;283:115593.
[19] Chen MT, Pandey M, Young B. Mechanical properties of cold-formed steel semi-oval hollow sections after exposure to ISO-834 fire. Thin-Walled Struct 2021;167: 108202.
[20] Chen MT, Pandey M, Young B. Post-fire residual material properties of cold-formed steel elliptical hollow sections. J Constr Steel Res 2021;183:106723.
[21] Gardner L, Cruise RB. Modeling of residual stresses in structural stainless steel sections. J Struct Eng ASCE 2009;135:42–53.
[22] Laubscher RF, Van Der Merwe P. Structural design in hot-rolled 3Cr12 sections. In: Proc, Stainless Steel Structures Int Experts' Seminar, Ascot, U.K. Steel Construction Institute; 2003. p. 93–100.
[23] ABAQUS. ABAQUS/standard user's manual. Version 6.17. Dassault Systemes Simulia Corp. USA; 2017.
[24] Kucukler M. In-plane structural response and design of steel I-section beam-columns at elevated temperatures. Structures 2022;39:1045–62.
[25] Kucukler M. Cross-section stability and design of normal strength and high strength steel I-sections in fire. Int J Struct Stab Dyn 2022:2250146.
[26] Chan TM, Gardner L. Compressive resistance of hot-rolled elliptical hollow sections. Eng Struct 2008;30:522–32.
[27] Gardner L, Chan TM. Cross-section classification of elliptical hollow sections. Steel Compos Struct 2007;7:185–200.
[28] Meng X, Gardner L. Simulation and design of semi-compact elliptical hollow sections. Eng Struct 2020;202:109807.
[29] Meng X, Gardner L, Sadowski AJ, Rotter JM. Elasto-plastic behaviour and design of semi-compact circular hollow sections. Thin-Walled Struct 2020;148:106486.
[30] Whitfield S. Hot vs. cold formed hollow sections. Struct Eng 2007;85(21):32–4.
[31] Gardner L, Saari N, Wang F. Comparative experimental study of hot-rolled and cold-formed rectangular hollow sections. Thin-Walled Struct 2010;48:495–507.
[32] EN 10219-2. Cold formed welded structural hollow sections part 2: tolerances, dimensions and sectional properties. Brussels: European Committee for Standardization (CEN); 2019.
[33] EN 10210-2, hot-finished structural hollow sections part 2: tolerances, dimensions and sectional properties. Brussels: European Committee for Standardization (CEN); 2019.
[34] H. T. Li, B. Young, Cold-formed high strength steel SHS and RHS beams at elevated temperatures, J Constr Steel Res 158;475–85.
[35] Meng X, Gardner L. Behavior and design of normal- and high-strength steel SHS and RHS columns. J Struct Eng 2020;146:04020227.
[36] Xing Z, Kucukler M, Gardner L. Local buckling of stainless steel I-sections in fire: finite element modelling and design. Thin-Walled Struct 2021;161:107486.
[37] Kucukler M. Local stability of normal and high strength steel plates at elevated temperatures. Eng Struct 2021;243:112528.
[38] Arrayago I, Real E, Gardner L. Description of stress-strain curves for stainless steel alloys. Mater Des 2015;87:540–52.
[39] Mirambell E, Real E. On the calculation of deflections in structural stainless steel beams: an experimental and numerical investigation. J Constr Steel Res 2000;54: 109–33.
[40] Rasmussen KJR. Full-range stress-strain curves for stainless steel alloys. J Constr Steel Res 2003;59:47–61.
[41] Design Manual for Structural Stainless Steel. 4th ed. Steel Construction Institute (SCI); 2017.
[42] Ala-Outinen T, Oksanen T. Stainless steel compression members exposed to fire. Research Notes 1864. Finland: Technical Research Centre of Finland (VTT); 1997.
[43] Chen J, Young B. Stress-strain curves for stainless steel at elevated temperatures. Eng Struct 2006;28(2):229–39.
[44] Gardner L, Insausti A, Ng KT, Ashraf M. Elevated temperature material properties of stainless steel alloys. J Constr Steel Res 2010;66(5):634–47.
[45] Gardner L, Bu Y, Francis P, Baddoo NR, Cashell KA, McCann F. Elevated temperature material properties of stainless steel reinforcing bar. Constr Build Mater 2016;114:977–97.
[46] Afshan S, Zhao O, Gardner L. Standardised material properties for numerical parametric studies of stainless steel structures and buckling curves for tubular columns. J Constr Steel Res 2019;152:2–11.
[47] Chen MT, Young B. Tensile tests of cold-formed stainless steel tubes. J Struct Eng 2020;146:1–13.
[48] Cruise RB, Gardner L. Strength enhancements induced during cold forming of stainless steel sections. J Constr Steel Res 2008;64:1310–6.
[49] Rossi B, Degée H, Pascon F. Enhanced mechanical properties after cold process of fabrication of non-linear metallic profiles. Thin-Walled Struct 2009;47(12): 1575–89.
[50] Ala-Outinen T. Fire resistance of austenitic stainless steels Polarit 725 (EN 1.4301) and Polarit 761 (EN 1.4571). VTT research notes 1760. Espoo (Finland); 1996.
[51] McCann F, Gardner L, Kirk S. Elevated temperature material properties of cold-formed steel hollow sections. Thin-Walled Struct 2015;90:84–94.
[52] Quan C, Kucukler M. Simulation and cross-section resistance of stainless steel SHS and RHS at elevated temperatures. Thin-Walled Struct 2023;189:110849.
[53] EN 1993-1-5. Eurocode 3: design of steel structures part 1-5: plated structural elements. Brussels: European Committee for Standardization; 2006.
[54] Silvestre N, Gardner L. Elastic local post-buckling of elliptical tubes. J Constr Steel Res 2011;67:281–92.
[55] Jandera M, Gardner L, Machacek J. Residual stresses in cold-rolled stainless steel hollow sections. 2008;64:1255–63.
[56] Rasmussen KJR, Hancock GJ. Design of cold-formed stainless steel tubular members. I: columns. J Struct Eng ASCE 1993;119:2349–67.
[57] Huang Y, Chen J, He Y, Young B. Design of cold-formed stainless steel RHS and SHS beam–columns at elevated temperatures. Thin-Walled Struct 2021;165.
[58] Kucukler M. Compressive resistance of high-strength and normal-strength steel CHS members at elevated temperatures. Thin-Walled Struct 2020;152:106753.
[59] Buchanan C, Real E, Gardner L. Testing, simulation and design of cold-formed stainless steel CHS columns. Thin-Walled Struct 2018;130:297–312.
[60] Scullion T, Ali F, Nadjai A. Experimental study on performance of elliptical section steel columns, under hydrocarbon fire. J Constr Steel Res 2011;67:986–91.
[61] Scullion T, Ali F, Nadjai A. Finite element numerical evaluation of elliptical hollow section steel columns in fire. Thin-Walled Struct 2012;55:22–36.
[62] Tondini N, Rossi B, Franssen JM. Experimental investigation on ferritic stainless steel columns in fire. Fire Saf J 2013;62:238–48.
[63] Tondini N, Hoang VL, Demonceau JF, Franssen JM. Experimental and numerical investigation of high-strength steel circular columns subjected to fire. J Constr Steel Res 2013;80:57–81.
[64] Quan C, Kucukler M. Cross-section resistance and design of stainless steel CHS and EHS at elevated temperatures. Eng Struct 2023;285:115996.
[65] EN 1993-1-1:2005 + A1: 2014. Eurocode 3: design of steel structures – part 1-1: general rules and rules for buildings. Brussels: European Committee for Standardization; 2014.

[66] EN 1993-1-4:2006 + A1: 2015. Eurocode 3: design of steel structures – part 1-4: general rules – supplementary rules for stainless steels. Brussels; 2015.
[67] UK NA to EN 1993-1-4. UK National Annex to Eurocode 3. Design of steel structures: part 1–4: general rules—supplementary rules for stainless steels. BSI; 2015.
[68] Ayrton W, Perry J. On struts. Engineer 1886;62:464–5.
[69] Robertson A. The strength of struts. Inst Civ Eng (ICE) – Sel Eng Pap 1925;1(28):1–55.
[70] Xing Z, Kucukler M, Gardner L. Local buckling of stainless steel plates in fire. Thin-Walled Struct 2020;148:106570.
[71] Timoshenko SP, Gere JM. Theory of Elastic stability. New York: McGraw-Hill; 1961.
[72] Kempner J. Some results on buckling and post buckling of cylindrical shells. Collected papers on instability of shell structures. NASA TND 1962;1510:173–86.
[73] Gardner L, Nethercot DA. Experiments on stainless steel hollow sections-part 2: member behaviour of columns and beams. J Constr Steel Res 2004;60:1319–32.
[74] Li S, Zhao O. Local–flexural interactive buckling behaviour and resistance of press-braked stainless steel slender channel section columns. Eng Struct 2022;270:114871.
[75] Couto C, Vila Real P, Lopes N, Zhao B. Numerical investigation of the lateral-torsional buckling of beams with slender cross sections for the case of fire. Eng Struct 2016;106:410–21.
[76] Kruppa J. Eurocodes–fire parts: proposal for a methodology to check the accuracy of assessment methods. CEN TC 250. Horizontal Group Fire, Document; 1999. p. 99–130.
[77] Talamona D, Franssen M, Schleich B, Kruppa J. Stability of steel columns in case of fire: numerical modelling. J Struct Eng 1997;123(6):713–20.
[78] Franssen J, Schleich J, Cajot L. A simple model for the fire resistance of axially loaded members – comparisons with experimental results. J Constr Steel Res 1996;37:175–204.